Review

A review of lithium-ion battery safety concerns: The issues, strategies, and testing standards

Yuqing Chen [a,c,1], Yuqiong Kang [b,1], Yun Zhao [c,*], Li Wang [c], Jilei Liu [a,*], Yanxi Li [d], Zheng Liang [d,*], Xiangming He [c], Xing Li [e], Naser Tavajohi [f], Baohua Li [b,*]

[a] College of Materials Science and Engineering, Hunan Province Key Laboratory for Advanced Carbon Materials and Applied Technology, Hunan University, Changsha, 410082, China
[b] Engineering Laboratory for Next Generation Power and Energy Storage Batteries, Graduate School at Shenzhen, Tsinghua University, Shenzhen 518055, Guangdong, China
[c] Institute of Nuclear & New Energy Technology, Tsinghua University, Beijing 100084, China
[d] Department of Materials Science and Engineering, Stanford University, Stanford, CA 94305, USA
[e] Technical Center, SAIC Motor, Shanghai 201804, China
[f] Department of Chemistry, Umeå University, Umeå 90187, Sweden

ARTICLE INFO

ABSTRACT

Efficient and reliable energy storage systems are crucial for our modern society. Lithium-ion batteries (LIBs) with excellent performance are widely used in portable electronics and electric vehicles (EVs), but frequent fires and explosions limit their further and more widespread applications. This review summarizes aspects of LIB safety and discusses the related issues, strategies, and testing standards. Specifically, it begins with a brief introduction to LIB working principles and cell structures, and then provides an overview of the notorious thermal runaway, with an emphasis on the effects of mechanical, electrical, and thermal abuse. The following sections examine strategies for improving cell safety, including approaches through cell chemistry, cooling, and balancing, afterwards describing current safety standards and corresponding tests. The review concludes with insights into potential future developments and the prospects for safer LIBs.

© 2020 The Authors. Published by ELSEVIER B.V. and Science Press on behalf of Science Press and Dalian Institute of Chemical Physics, Chinese Academy of Sciences. This is an open access article under the CC BY-NC-ND license (http://creativecommons.org/licenses/by-nc-nd/4.0/).

Contents

---

* Corresponding authors.
   E-mail addresses: zhao.yun@sz.tsinghua.edu.cn, yzhao.zjut@hotmail.com (Y. Zhao), liujilei@hnu.edu.cn (J. Liu), lianzhen@stanford.edu (Z. Liang), libh@sz.tsinghua.edu.cn (B. Li).
  [1] These authors contribute to this work equally.

1. Introduction

Lithium-ion batteries (LIBs) have raised increasing interest due to their high potential for providing efficient energy storage and environmental sustainability [1]. LIBs are currently used not only in portable electronics, such as computers and cell phones [2], but also for electric or hybrid vehicles [3]. In fact, for all those applications, LIBs' excellent performance and energy density have made them increasingly popular [4]. In addition, the battery market for portable electronics is currently dominated by LIBs because of their inherent advantages over other battery systems, such as high specific capacity and voltage, no memory, excellent cycling performance, little self- discharge, and wide temperature range of operation [5,6]. Further expansion of the LIB market and its large-scale implications in EVs are currently significantly hindered, however, by their limited safety performance [7-11]. In recent years, tons of LIBs have been recalled due to explosion and fire accidents [12-15], resulting in severe economic issues for related market sectors and significantly damaging the reputation of LIBs [16-19]. Consequently, increasing attention is being paid to LIB safety issues and a large number of safety strategies are being developed.

Battery safety is profoundly determined by the battery chemistry [20-22], its operating environment, and the abuse tolerance [23,24]. The internal failure of a LIB is caused by electrochemical system instability [25,26]. Thus, understanding the electrochemical reactions, material properties, and side reactions occurring in LIBs is fundamental in assessing battery safety. Voltage and temperature are the two factors controlling the battery reactions. Safety accidents are accompanied by continuous heat and gas generation, which causes battery rupture and ignition of the combustible materials [27-29]. The external environment (which controls the temperature, voltage, and electrochemical reactions) is the leading cause of internal disturbances in batteries [30]. Thus, the environment in which the battery operates also plays a significant role in battery safety.

Safety standards and related tests have been developed to analyze battery performance and influential factors to meet the required safety demands. For example, GB/T 31485–2015 standard safety tests [31] were established in China, thereby helping the implementation of stringent standards for LIBs produced and used in China. These strict and vigorous battery safety tests ensure no future safety problems under normal working conditions. Stable LIB operation under normal conditions significantly limits battery damage in the event of an accident. As a result of all these measures, current LIBs are much safer than previous generations, though additional developments are still needed to improve battery safety even further.
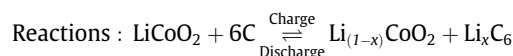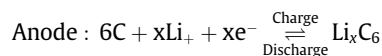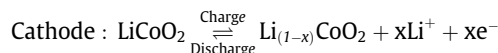
Several high-quality reviews papers on battery safety have been recently published, covering topics such as cathode and anode materials, electrolyte, advanced safety batteries, and battery thermal runaway issues [32-35]. Compared with other safety reviews, the aim of this review is to provide a complementary, comprehensive overview for a broad readership with special interest in root causes of safety incidents, strategies to improve safety on different levels, as well as a systematic introduction to various safety standards and test specifications. This review summarizes various aspects of LIB safety, with the main goal of describing the issues, strategies, and testing standards for checking and improving such safety. It starts with a brief introduction to LIB structure and materials; we then summarize the processes leading to LIB thermal runaway under mechanical, electrical, and thermal abuse conditions; afterwards we propose solutions for improving battery safety, in normal and abuse conditions, such as adjusting the cell chemistry, as well as improving cell cooling and cell balancing; lastly, we review LIB safety standards and applicable tests worldwide. The review then concludes with an overview of potential future developments and strategies for improving LIB safety.

2. LIB working principle

LIBs typically consist of four major parts: cathode, anode, separator, and electrolyte [36]. Cathodes and anodes are the charge carriers contributing to LIB energy storage and release. The separator physically divides the electrodes to prevent internal short-circuits while allowing Li^+ flow. The electrolyte carries ions, including Li^+. The malfunction of these parts, together or individually, can negatively affect LIB safety. When operating, the electrodes produce heat, which might become uncontrollable during battery malfunction [37]. If a separator is damaged, LIB processes transit from controlled to uncontrolled electrochemical reactions, with significant heat generation [38]. In such cases, the electrolyte acts as a fuel supply for further heat generation, so appropriate safety regulations, which can be established by researching the controllable and uncontrollable factors in battery failures, are essential for improving LIB safety performance.

The working mechanism of typical LIBs is shown in Fig. 1(a), using a $LiCoO_2$/graphite cell as an example [36]. During charging, Li^+ de-intercalates from the cathode materials ($LiCoO_2$, in this case), diffuses into the electrolyte and moves through the separator nano-pores to intercalate into the anode material. Meanwhile, electrons move in the opposite direction through the external circuit to maintain electro-neutrality. During discharging, Li^+ ions transport from the anode side back to the cathode. The charge and discharge reactions are as follows:

$$\text{Cathode}: LiCoO_2 \underset{Discharge}{\overset{Charge}{\rightleftharpoons}} Li_{(1-x)}CoO_2 + xLi^+ + xe^-$$

$$\text{Anode}: 6C + xLi_+ + xe^- \underset{Discharge}{\overset{Charge}{\rightleftharpoons}} Li_xC_6$$

$$\text{Reactions}: LiCoO_2 + 6C \underset{Discharge}{\overset{Charge}{\rightleftharpoons}} Li_{(1-x)}CoO_2 + Li_xC_6$$

Shuttling of Li^+ during battery operations generates a significant amount of heat, which is released as a result of the Joule heat and the chemical energy of the charge/discharge process [39]. This heat release is a normal part of battery operation, but if the generated
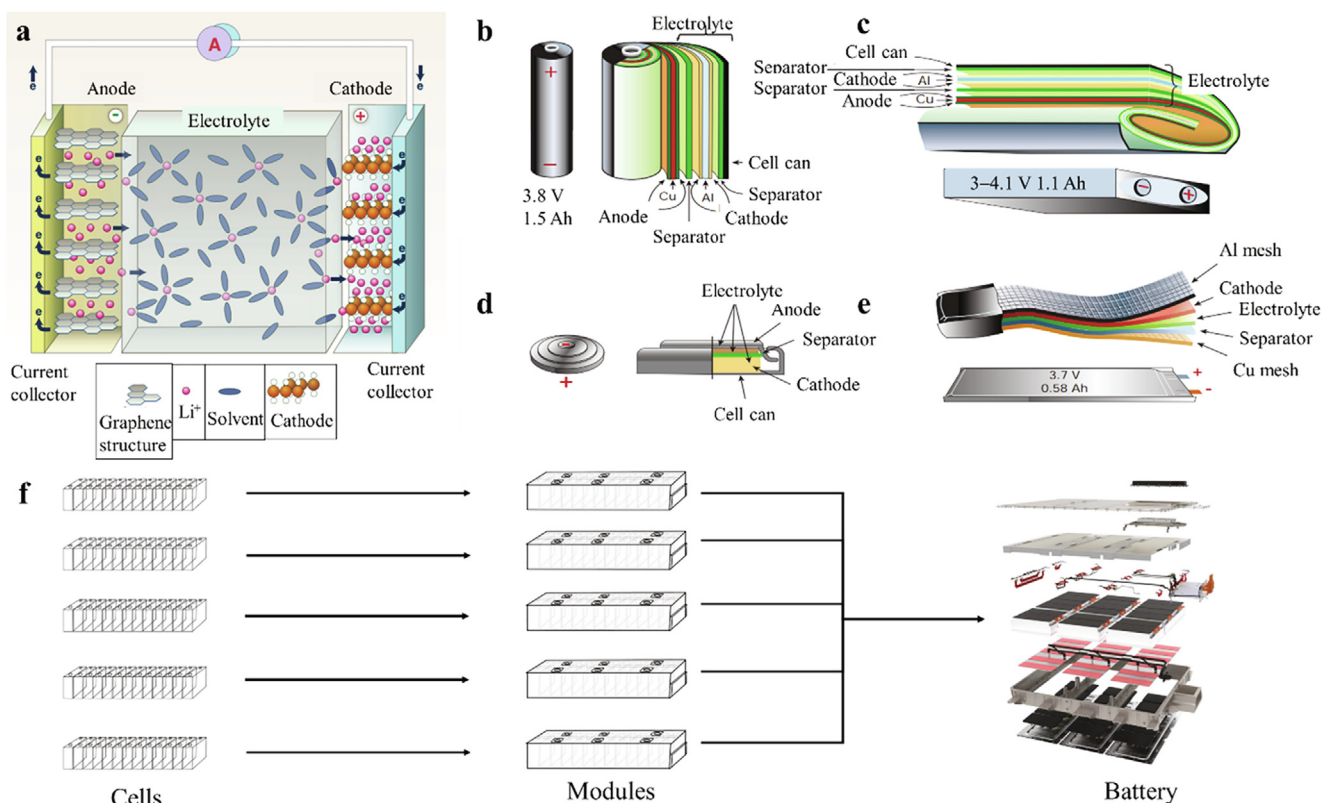
Fig. 1. (a) Schematic diagram of the fundamental structure of a LIB cell, which is the same for different cell types [36]. Copyright (2011) American Association for the Advancement of Science [36]. Cell types: (b) cylindrical cell; (c) prismatic cell; (d) coin cell; (e) pouch cell. Copyright (2001) Macmillan Magazines Ltd [41]. (f) Schematic diagram of the relationship between cell, module, and battery.

heat has no efficient dissipation path in certain charge/discharge states the battery would become excessively hot, which seriously compromise battery safety [40].

The four most commonly-used types of cell in LIBs are cylindrical, prismatic, coin, and pouch cells (Fig. 1b-e) [41]. Cylindrical cells include both high- and low-capacity cells. Due to the high
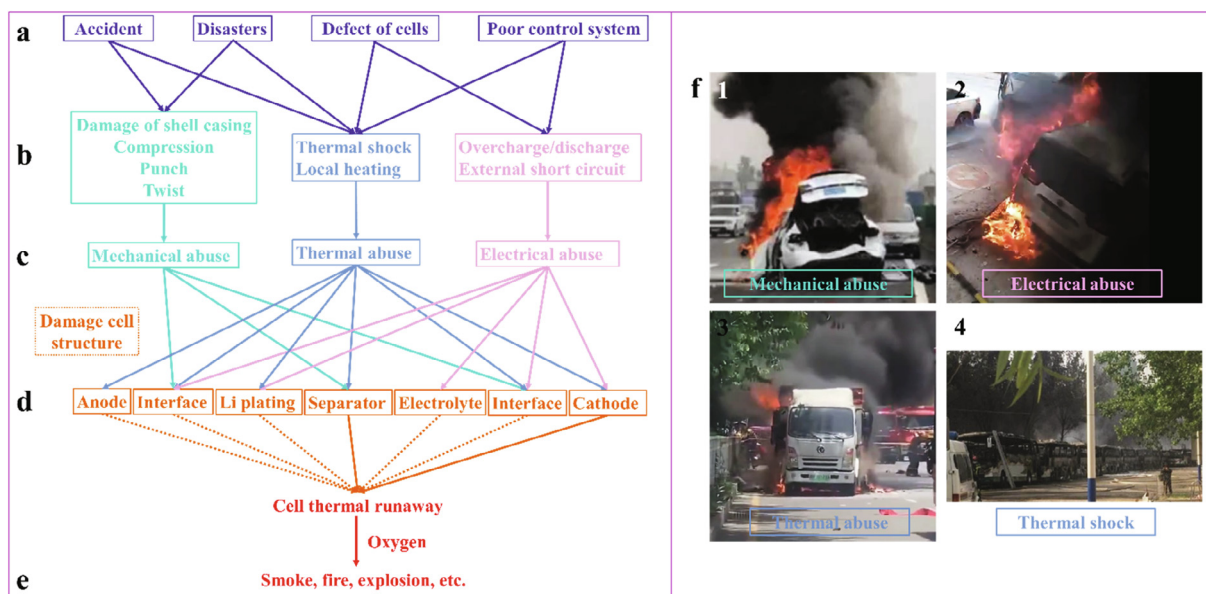

Fig. 2. An overview of battery safety issues. Battery accidents, disasters, defects, and poor control systems (a) lead to mechanical, thermal abuse and/or electrical abuse (b, c), which can trigger side reactions in battery materials (d). Broken separators and oxygen released from cathodes are the main reasons for cell thermal runaway, which can generate smoke, fires, and explosions with the help of oxygen from air (e). (f) Collision (mechanical abuse), charging (electrical abuse), self-ignition (thermal abuse) and thermal shock (thermal abuse) caused electric vehicle fires. (1) The collision process causes the battery to squeeze, and the area with strong stress is damaged, resulting in the internal short-circuit or the casing rupture, which can cause thermal runaway of batteries. (2) During the abused charging process, the heat generation is too late to diffuse, resulting in heat accumulation inside the battery, leading to thermal runaway of batteries. (3) During the operation of the battery, if the heat generated is too late to diffuse, it is easy to cause the battery thermal runaway. (4) When the battery receives a local thermal shock, it is easy to cause the battery to catch fire. The fire of an electric vehicle will cause the burning of electric vehicles in the nearby area.

impedance of high-capacity cylindrical cells, low-capacity cells are used in most applications. Prismatic cells have large capacities, so fewer cells need to be connected to assemble a battery pack with the required capacity, with benefits for overall system stability [42]. Coin cells are small and typically used for laboratory material testing. The pouch design does, however, offer flexibility in terms of matching the cell to a specific device shape. This advantage has allowed pouch cells to achieve a majority market share.

From the perspective of safety, a larger cell size typically makes it challenging to ensure its overall reliability. The safety risk increases in the order of cylindrical cells < pouch cells < prismatic cells. The heat dissipation of prismatic cells is poor, which makes the cooling process and cell assembly more challenging. The small size, lower energy stored of cylindrical cells as well as the gap between each single cell all together enable the cylindrical-based battery packs with better heat dissipation. The shell casing of cylindrical and prismatic cells is metallic and can withstand high pressure. In contrast, the aluminum-plastic composite film in pouch cell's shell casings deforms easily and withstands less pressure [43]. Once there is an internal safety issue, a pouch cell battery will swell and bulging will occur at the weakest point on the battery surface, which may lead to a fire but not an explosion. Currently, when selecting types of cell, automakers mainly consider their own battery integration technology and the balance of overall battery performance. For example, cylindrical cells are used in Tesla S3 models, prismatic cells in BYD Tang, Song, and Qin models, and pouch cells in SAIC Motor's ROEWE R ER6 model.

In practical, hundreds to thousands cells are typically combined (in parallel and in series) into one battery pack to obtain specific voltage and capacity (Fig. 1f) [44]. For example, the Tesla EV contains about 7000 cylindrical cells with a total voltage and capacity of 400 V and 85 kWh, respectively [45]. Battery management in such a large battery pack is pretty challenging for battery safety.

3. LIB safety issues

Even under normal operating conditions, battery-generated heat cannot be entirely removed, especially on hot days or in a large battery pack [40]. Rising battery temperature would trigger other undesirable parasitic reactions, causing thermal runaway, where battery heat generation cannot be controlled [46]. During mechanical (damage to shell casing, compression, punching, and twisting of cells), electrical (overcharge/discharge and short circuit), and thermal abuse (thermal shock and local heating) situations, which could occur during accidents, thermal runaway will occur even quicker (Fig. 2a-c, and f) [47–49]. Understanding LIB performance in unsafe conditions is critical, therefore, for the production of safer cells.

3.1. Safety issues caused by undesirable chemical reactions

In the normal voltage and temperature range, only Li^+ shuttle occurs in the electrolyte during the insertion/extraction cycles at the cathode and anode. At high-temperature and high-voltage conditions, the electrochemical reactions become more complex, including decomposition of the solid electrolyte interface (SEI) film, oxygen release at the cathode side, and additional electrolyte/electrode parasitic side reactions [50]. SEI film decomposition and interfacial reactions initially accelerate the temperature increase, thereby increasing risks of oxygen release from the active cathode materials [51]. These reactions eventually lead to LIB thermal runaway, which causes battery rupture and explosion due to the reaction of hot flammable gases from the battery with the ambient oxygen [52].

3.2. Thermal runaway

Thermal runaway is the most detrimental LIB safety issue. Fig. 2 shows the origins of thermal runaway in batteries, including side reactions of electrolyte, cathode, anode, and interfacial reactions at the surface of electrodes and Li plating. These side reactions are triggered by mechanical, thermal, and electrical abuse. Breakage of the separator and the oxygen evolution from the cathode side are the root causes to batteries' thermal runaway (as shown in the solid line of Fig. 2d).

There are five types of causes for this phenomenon, which are illustrated in Fig. 2. The first type is uncontrollable internal heat generation, which causes oxygen release from the cathode material, leading to numerous side reactions [37,53]. In the second type, separator defects (due to thermally-induced shrinkage or mechanical damage) create short circuits in the battery and rapid discharge of the energy stored in it [54], accompanied by undesirable chemical chain reactions and release of massive amounts of heat. The third type is electrical abuse [55]. Electrolyte decomposition, especially in a high state of charge (SOC), occurs at the cathode interface. This leads to heat accumulation and consequently release of oxygen from the cathode and damage to the separator. The fourth type consists of electrochemical side reactions caused by local thermal abuse. If the heat generated during normal LIB operations cannot be dissipated quickly enough, the separator in that specific place will shrink or rupture [41,56]. The fifth type occurs during mechanical battery damage, which causes short circuits and/or air to penetrate the battery [57]. The main causes of battery safety accidents among these five categories are shortcircuiting due to separator damage, electrical abuse, and mechanical abuse [11,58].

3.3. Safety issues caused by mechanical abuse

Due to the high energy density of LIBs, local damage caused by external influences, for example in case of collisions, will release a significant amount of heat, which can easily cause thermal runaway. As a result their safety risk is high. As the number of EVs (containing LIBs) on the roads continues to increase, safety concerns over battery behavior during potential vehicle collisions are becoming more prominent. A moving car's battery experiences local forces, which in extreme cases can cause local damage to LIBs [59].

Each cell includes a shell (made of aluminum plastic film or steel) and a jelly roll composed of cathode, anode as well as separator. Under external forces, the weakest point of this cell is prone to damage. Numerous battery ignition cases are caused by mechanical abuse (mainly collisions) in electric vehicles every year, but few details are publicly reported. Current research on mechanical abuse focuses on theoretical simulation and experimental verification to provide reference data for battery manufacturers. Therefore, in this section, we mainly discuss the impact of different kinds of mechanical abuse of batteries, largely based on theoretical simulations, to provide indications of their effects for readers.

The outer casing provides a cell's first level of thermal and mechanical protection. The shell casing needs to withstand mechanical force and not break, and ensure that the internal structure is not damaged under certain deformation conditions [60]. The mechanical behavior of the shell casing is an important aspect of the overall LIB mechanical behavior, as it is the most vulnerable point during safety accidents, so it should be understood and taken into account during LIB materials' design and consideration [57]. Upon damage to it, air directly enters the battery system, reacting with the active components and electrolytes.
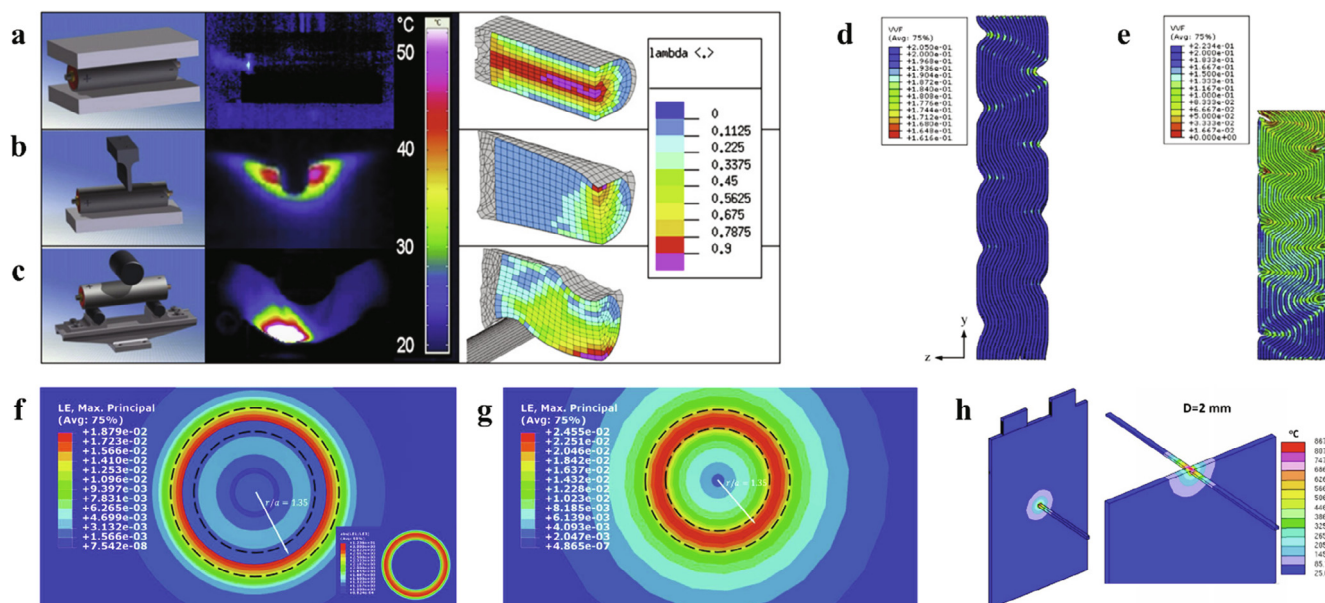
Fig. 3. Comparison of short-circuit locations for different cells observed experimentally as well as their corresponding model predictions under various breakage cases indicated: (a) "radial crushing", (b) "indentation", (c) "bending". Copyright (2012) Elsevier [63]. Void space fraction distributions under nominal strains of (d) 8.5% and (e) 34% of the constrained compression simulation. Copyright (2013) Elsevier [64]. Stress distribution in the separator layer by sumulations (f) before twisting and (g) after 12° angle twisting. Copyright (2014) Elsevier [65]. (h) The temperature distribution of pouch cell during the nail penetration process [68].

Even when the shell casing is only deformed, LIB internal components might still be severely damaged: metallic current collectors and separators with insufficient flexibility would break, causing direct contact between the electrodes [61]. When the heat generated by the high-energy density LIB after a localized short circuit is sufficient to trigger other internal short circuits in the area, thermal runaway occurs in overall battery [62].

The distribution of internal stresses in a cell varies depending on the form of mechanical abuse [63]. Such stresses in certain areas of the battery could cause internal short circuits. Fracture prediction and the possible internal short circuit inhibition are proved to be achieved by finite element simulations on cell's cylindrical casing as well as the cell housing. The experimental results agreed with the theoretical results: short circuit initiated at end of the cylinder, close to the connection section of battery electrode, which was confirmed by an infrared image (Fig. 3a). Indentation damage caused the short circuit to appear close to the punch area (Fig. 3b), whereas bending mechanical damage caused the short circuit to form on the cylinder casing surface opposite the point of force (Fig. 3c).

Cell damage by squeezing deformation can tear the separator, causing the electrodes to come into direct contact. The resulting damage and observations are quite different to those from short circuiting caused by nail penetration. Pan et al. modeled the changes in a LIB cell subjected to in-plane compression [64]. During the deformation under a 8.5% of nominal strain, no voids could be observed at the bending site along shear band outer boundaries (Fig. 3d). At the final step of the compression, when the nominal strain reached 34%, the fraction of void volume at top region of the sample decreased compared with that near the bottom (Fig. 3e).

Shear strain could be introduced to the cell by a slight twisting, which in turn increases the tension zone maximum strain and stimulates polymer failure. Wang group demonstrated that under a 12° twisting the maximum strain increased by over 77% in the tension zone (Fig. 3f and g) [65]. Under this condition, slip and stick region were created due to partial slipping of the cell as well as contact surface.

Under more extreme conditions, damage similar to that observed during nail penetration tests occurs: the separator becomes pierced and a small amount of air near the nail penetrates the cell, initiating vigorous exothermic oxidation reactions, with excessive and heat that is difficult to dissipate, which increases the temperature of nearby areas (Fig. 3h) [66-68]. The ideal situation is when the nail penetration generates only a small amount of heat and self-passivation of the electrode material interface occurs quickly, thereby preventing a battery fire [67]. Wang et al. showed that during LIB penetration with a small nail or during indentation, the metallic casing and the nail itself acted as heat sinks [68]. The same test performed with a LIB with higher capacity and voltage resulted in more significant damage. LIB nail penetration tests of $LiCoO_2$ cell carried out by Doh et al. resulted in a fire and sudden voltage drop to 0 V, with the temperature increasing sharply to 420 °C [69]. At the moment of penetration, a very high discharge current overflow from the battery occurred, generating high Joule heat, which shrank the battery separator. Nature of the active cathode material, as well as cell's specific capacity and state of charge (SOC) profoundly influence the results of nail penetration test. Thus, the targeted design of the battery structure, or its enhancements, and incorporation of built-in protective measures will dramatically improve LIB safety during use.

3.4. Safety issues induced by electrical abuse

When a battery is in an overcharge or over-discharge state, or is undergoing an external short circuit, it experiences electrical abuse, and a series of undesirable electrochemical reactions occurs in it.

There are many reasons for battery overcharging. One of the main reasons is the inconsistency of battery cells. If the voltage of any battery cell cannot be effectively monitored by the management system, there will be risks of its overcharging. Since excess energy is stored into the battery, overcharging is very dangerous. Typically, all batteries are first charged to a specific SOC, but some batteries initially have higher SOC before charging. Thus, such batteries would become overcharged if they are charged any further
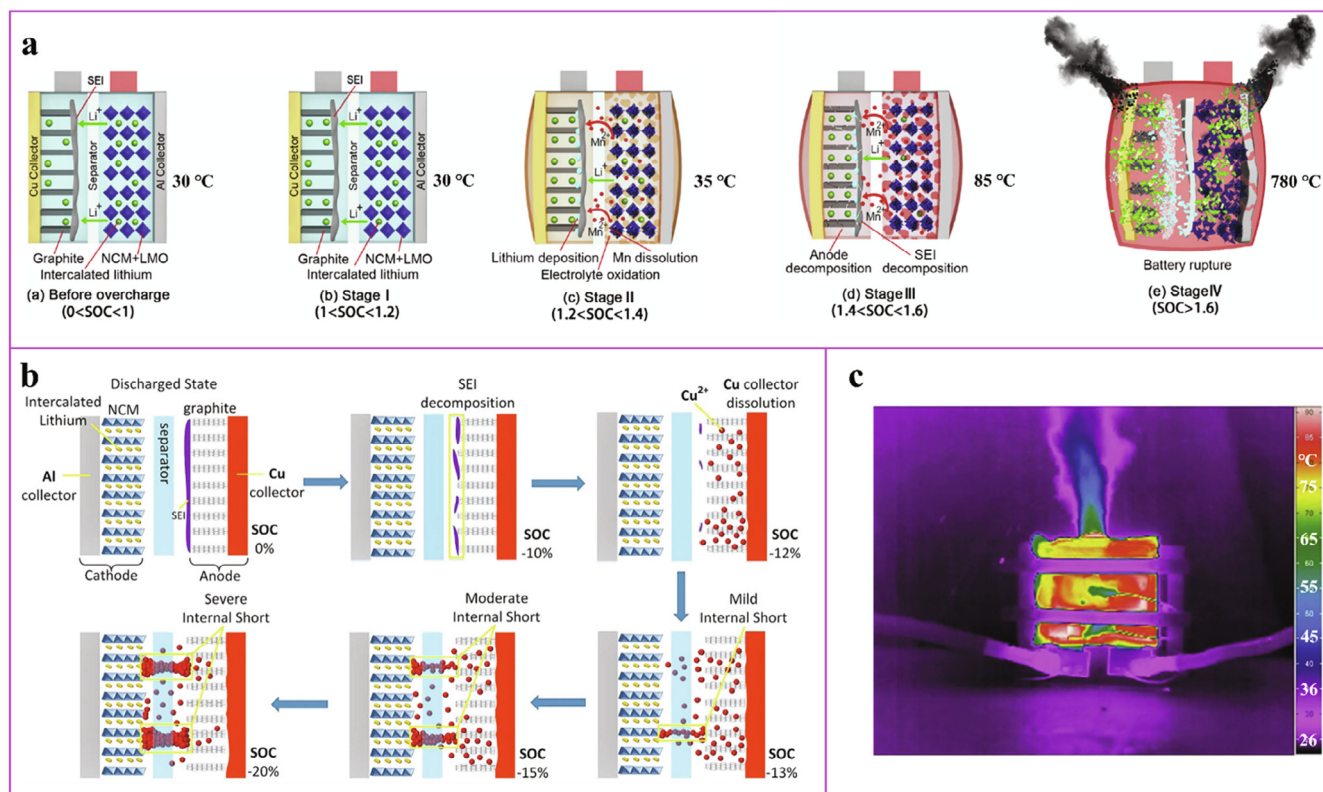
Fig. 4. Schematic presentation of the (a) overcharge and (b) over-discharge process. Copyright (2017) Elsevier [55]. Copyright (2016) The Author(s) [76]. (c) Infrared radiation image taken when cell rupture during a short circuit test. Copyright (2017) Elsevier [79].

[70]. Overcharge first causes electrolyte decomposition at the cathode interface [71]. This reaction slowly increases the battery temperature. Subsequently, excessive Li$^+$ deintercalation from the cathode occurs. The cathode material becomes unstable and start to release oxygen, while excess Li$^+$ deposits on the anode to form Li dendrite [72]. Heat and gas generation during the side reactions would lead to safety accidents, such as cell overheating and rupture [73]. Ouyang et al. summarized the overcharge process of a 40 Ah LIB containing Li$_y$Ni$_{1/3}$Co$_{1/3}$Mn$_{1/3}$O$_2$(NCM) + Li$_y$Mn$_2$O$_4$ (LMO) composite cathode and graphite anode (Fig. 4a) [55]. In stage I, the battery voltage increased steadily and exceeded its nominal cut-off voltage, marking the beginning of an overcharge process. In stage II, when the battery was overcharged by 1.2 V above full SOC, side reactions began to occur inside the battery. The battery temperature rose even more rapidly in stage III and the battery started to swell. In stage IV, the battery casing ruptured, which damaged the separator and caused LIB thermal runaway. Charging rate is often the most significant factor affecting overcharge, as the overcharging current density determines the rate of heat generation by the battery reactions: the higher the current, the more heat is generated per unit time, thereby increasing the risks of uncontrollable LIB behavior.

The principle of over-discharge is similar that of over-charge. Some cells reach the set state of discharge (SOD) in advance. Thus, an over-discharge occurs if a cell is forced to continue to discharge [74]. Forced over-discharge continuously releases Li$^+$ from the anode, which change the graphite structure and destroy the SEI. At very deep SOD, a copper current collector is oxidized, with the released copper ions potentially being deposited on the cathode surface [75]. Too much copper deposition results in the short-circuit of cell. The over-discharge profile of a 25 Ah commercial LIB pouch cell containing a NMC-based cathode and a graphite-based anode can be described by three stages based on observed

voltage variations (Fig. 4b) [76]. During stage I (up to 11% below SOD in the cited study), the voltage first drops rapidly due to Li$^+$ deintercalation from the anode to intercalate into the cathode. During stage II (up to 20% below SOD), Cu foil oxidization leads to a stable voltage. During the third stage, involving extensive SOD, the voltage asymptotically decreases to 0 V due to short-circuiting caused by Cu dendrite. Li et al. showed that SEI dissolution is the main reason for degradation in over-discharge conditions at low voltages, as well as for dissatisfactory cycling performance [77].

An external short circuit occurs when a cathode and an anode of the same cell are in direct contact through a conductor. In such cases, instead of decoupled electron and ion transportation, both electron and ion transfer occur at the same place and Li$^+$ migrates quickly inside the cell, rapidly discharging the battery. During a safety accident, a LIB cathode and anode might indeed come into contact, releasing the heat relatively evenly and quickly [78]. It is found that the complicated short-circuit behavior could be divided by three steps, as shown by Kriston et al. [79]. In the first step, a rapid discharge under 274C was observed. In the second step, the discharge rate was reduced to 50C – 60C, and mass transport was the limiting factor. At the same time, cell temperature ramped up to 77 – 121 °C and the cell eventually ruptured, causing the electrolyte's leakage (Fig. 4c). At the final stage, the cell current continued to drop to the fading voltage. The ratio of external to internal resistance after normalization had profoundly effect on the discharge rate.

Overcharge is the most dangerous types of electrical abuse and one of the most frequently observed reasons for LIB safety accidents. The other two types of electrical abuse, over-discharge and external short circuiting, are relatively benign and do not cause instant and fast-developing accidents. They can, however, still impair a LIB's state of health (SOH).

Table 1
Temperature ranges and enthalpies of various exothermic reactions occurring in LIBs.

Reactions	Temperature range (℃)	Enthalpy (J/g)	Ref.
SEI decomposition	100–130	186–257	85,86
LiC_6/electrolyte	110–290	1460–1714	87
LiC_6/PVDF	220–400	1100–1500	88
Li_xCoO_2 decomposition	178–250	146	89
$Li_xNi_{0.8}Co_{0.2}O_2$ decomposition	175–340	115	90
Li_xCoO_2/electrolyte	167–300	381–625	91
$Li_xNi_{0.8}Co_{0.2}O_2$/electrolyte	180–230	600–1256	92
Electrolyte decomposition	225–300	155–258	93

3.5. Safety issues caused by thermal abuse

In thermal abuse situations, a battery experiences thermal shock, or its local temperature is too high [80]. Battery fires might occur during electric vehicle charging or if nearby vehicles are on fire. Combustibles in the air (such as very flammable pollen grains or airborne seeds, flowers or leaves) in the vicinity of a malfunctioning battery might ignite if they are very close to or in contact with a hot battery, or a spark, setting everything around them on fire.

Localized high-temperature areas within a battery are typically related to its design. Poor LIB design leads to high impedance at the metal contacts or uneven heat dissipation, as manifested by the non-uniform temperature distribution observed in a LIB under thermal shock [81], simulated by placing it in an oven at 155 °C for 1200 seconds [47]. Since the elevated surrounding temperature caused exothermic reactions, the temperature distribution within the battery was more associated with the heat generated from these reactions than with the thermal energy distribution resulting from the elevated surrounding temperature. The highest temperature was observed at the center. The non-uniformity of the temperature distribution became more apparent with increased storage time. After 3600 seconds under these conditions, thermal runaway occurred in the cell.

In theory, battery cycling cannot cause safety accidents because the heat generated during normal anodic and cathodic reactions is insufficient to cause a sharp temperature increase. In reality, however, the electrode heat release rate is often higher than its cooling rate. Heat dissipation of a LIB depends on its external surface area and geometry. Heat dissipation by radiation helps to alleviate some of the generated heat. As a result, some of the heat remains stored inside the battery. At some point, if this heat continues to accumulate instead of being dissipated, exothermic side reactions start to occur, further concentrating thermal stress [82]. Table 1 shows the temperature ranges and enthalpy of the typical exothermic reactions occurring in LIBs [83–93]. Thermal stress and pressure build-up (due to the release of volatile side-products of these parasitic reactions) cause the explosion.

4. Strategies for LIB safety improvements

Battery safety is determined by the active material and electrolyte chemistry, the speed of heat generation and dissipation, and the tolerance of external forces. On one hand, safety analysis should start with evaluating the electrode active materials, electrolytes, and separators, as these are the most controllable factors. On the other hand, strategies for alleviating the consequences of thermal and electrical abuse also need to be engineered into LIBs. Moreover, freshly-manufactured LIBs can be tested for safety before they are incorporated into devices.

Since undesirable and uncontrollable heat and gas generation from various parasitic reactions are the leading causes of LIB safety

accidents, efforts to improve battery safety need to focus on ways to prevent LIBs from generating excessive heat, keeping them working at a suitable voltage range, and improving their cooling rates.

4.1. Internal strategies for LIB safety improvements

Internal strategies include safety enhancement of each LIB component: active materials, separator, and electrolyte. Adding appropriate additives to any of these components might also improve LIB safety performance [91,92].

Cathode material needs to be chemically and structurally stable to maintain a controllable chemical reaction during lithiation and delithiation [53,93]. The heat release for common battery materials has been summarized [11], and its starting temperature for cathode materials has been found to follow the order $LiCoO_2$ (LCO) < $LiNi_xCo_yAl_zO_2$ (NCA) < $LiNi_xCo_yMn_zO_2$ (NCM) < $LiFePO_4$ (LFP) (Fig. 5a). A very popular active cathode material is $LiFePO_4$, which has an ordered olivine structure and strong P-O covalent bonds forming a three-dimensional structure with excellent thermodynamic and kinetic stability [94]. $LiFePO_4$ has low reactivity with typical organic electrolytes, so cathodes containing $LiFePO_4$ can have excellent cyclability [95,96]. Recently developed Ni- and Li-rich materials have better voltage and specific capacity than $LiFePO_4$ [97], but intense interface reactions, low-temperature oxygen release, and high local heat generation hinder their more widespread use. Between 2018 and 2020, NMC and LFP batteries accounted for approximately ∼ 60% and 11% of LIB-based EVs' total safety accidents, respectively [98]. Thus, many scientists and engineers believe that $LiFePO_4$ will remain the mainstream active cathode material during the coming decades [99]. For a battery of the same capacity, if the oxygen release temperature of its active cathode materials is below that of $LiFePO_4$, rigorous safety testing is recommended before using it in practical applications. LIBs containing Ni-rich Ni-Mn-Co-oxides need improved interface stability and electrolyte and separator systems to pass current safety test standards [100]. In penetration tests, pouch cell assembled using LFP-coated NMC333 material (LFP@NMC333) and graphite anode with 100% SOC reportedly passed, while violent fires occurred during the penetration of uncoated NMC333 cells. Moreover, coating NMC333 can increase the time required for thermal runaway by about 25%, which greatly improves the safety of the battery [101]. In addition, various factors, such as element doping, electrolyte film-forming additives, and high-voltage electrolyte additives, can improve the interface stability of the cathode material [102,103].

A separator is a porous polymer film. Its role is to separate the cathode physically from the anode but allow the ions to pass between them. Traditional separators are polyolefin-based porous membranes, which are thermally unstable and structurally fragile [104]. They shrink at elevated temperatures, causing LIBs containing such separators to fail current safety standards (Table 2). Thus, shrinkage resistance and prevention of the internal short-circuiting of the battery upon separator shrinkage, as well as the polyolefin separators' overall mechanical stability, need to be addressed [105–107]. Some modifications on commercial separators, including coating with ceramic particles or other materials with high thermal stability can effectively increase the temperature at which thermal degradation starts to about 250 °C [108,109]. In addition, new types of separator materials and structures have been developed, which can greatly improve battery safety, and some separators can even work normally at high temperatures [92,110,111].

Lithium plating in the anode is also a major problem affecting the safety of LIB, which is mainly caused by electrical and thermal abuse. Since the lithium insertion potential of the graphite anode (0.1 vs Li^+/Li) is very close to the deposition potential of metallic
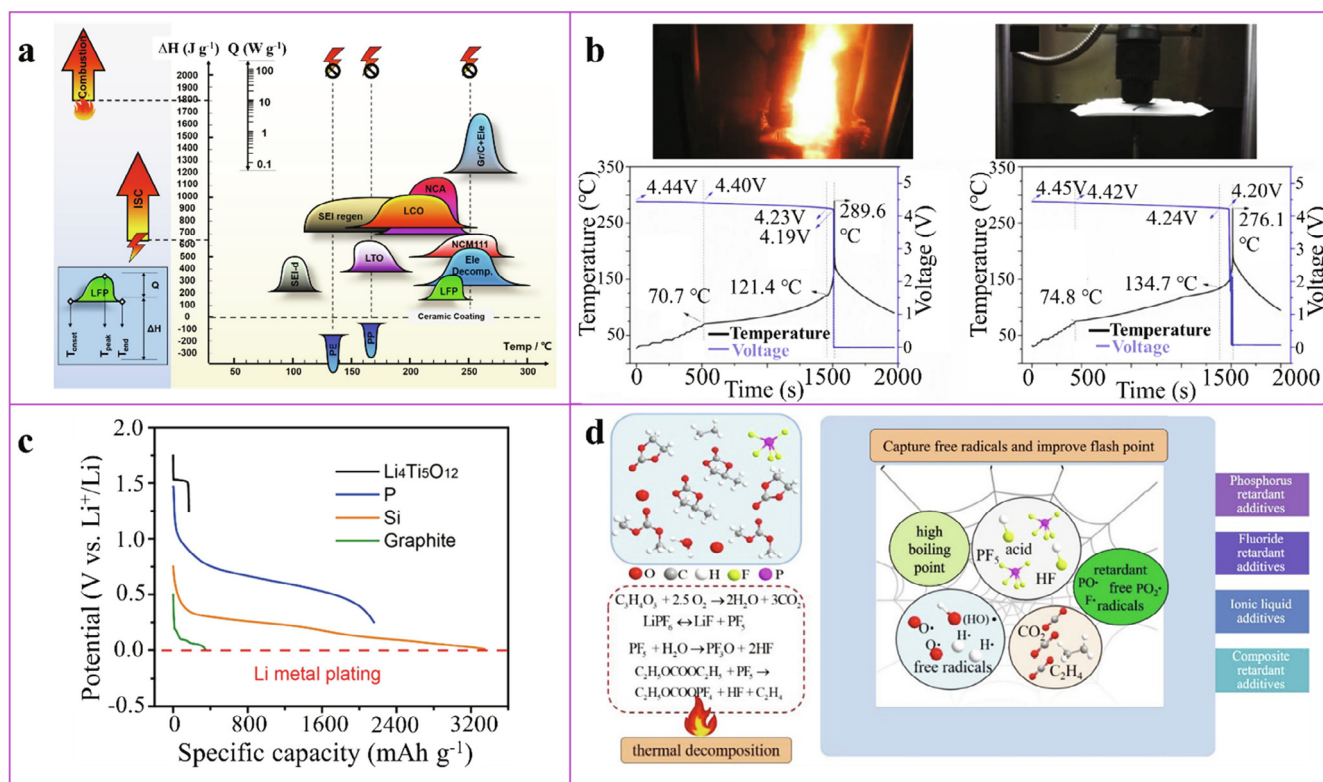
Fig. 5. (a) Diagram schematically illustrating energy release from a LIB. Copyright (2018) Elsevier [11]. (b) Results of nail penetration tests of NCM333/graphite and LFP@NMC333/graphite pouch cells at high SOC (images above, and thermal runaway curves below). Copyright (2014) Elsevier [101]. (c) Lithiation potential curves for typical anodes (Li$_4$Ti$_5$O$_{12}$, graphite, red P, and Si). Copyright (2019) Cellpress [114]. (d) Schematic diagram of flame-retarding additives for LIB. Copyright (2018) Elsevier [118].

Table 2
Shutdown temperatures and melting points of various polyethylene (PE), polypropylene (PP), and trilayer hybrid PP/PE/PP membranes.

Membrane composition	Shutdown temperature (°C)	Melting point (°C)
PE	130–133	139
PP	156–163	162
PP/PE/PP	134–135	165

lithium. Metallic lithium and electrolyte are unstable, and excessive metallic lithium deposition will cause the formation of dendrites to pierce the separator and cause battery short circuit. The most ideal solution at present is to develop anode materials with higher lithiation potential to reduce the risk of lithium deposition. Among them, Li$_4$Ti$_5$O$_{12}$ has a higher lithium insertion potential but a lower specific capacity (175 mAh g^{-1}), which will reduce the energy density of LIBs in practical applications [112]. Si and P have a high lithiation potential and a very high specific capacity [113,114]. They are theoretically very suitable as anode materials for next-generation lithium-ion batteries, but both of them have a large lithiation volume expansion (~300%) and still have challenge in practical applications. Through the nanometerization of materials, it has begun to be applied in practice [115].

Batteries containing traditional liquid organic carbonate-based electrolytes often combust or even explode when exposed to air (or other undesirable conditions) because of the extreme electrolyte flammability [116]. Furthermore, the poor thermal stability of these electrolytes causes their decomposition and reactions with the electrode's active materials [117]. If a flammability point or decomposition temperature can be increased, or fire-retarding additives can be added to decrease liquid electrolyte flammability, the drawbacks of the carbonate-based electrolytes would be significantly diminished. The combustion reaction is mainly composed

of free radical reactions. Therefore introducing a radical scavenger to the electrolyte can greatly lower the battery flammability. The currently reported electrolyte additives are mainly small molecules including phosphorus and fluorine species and ionic liquids, and the addition amount in the electrolyte is generally about 10% [118]. Implementation of solid-state electrolytes (based on polymers, glasses, or ceramic materials) [119-124], with their outstanding structural and thermal stability, can eliminate some of these adverse effects [125].

4.2. External strategies for LIB safety improvements

4.2.1. Cooling

High temperature operation and temperature inconsistency between battery cells will lead to accelerated battery aging, which trigger safety problems such as thermal runaway, which seriously threatens vehicle safety. A well-engineered built-in cooling system is an essential part of LIB safety since it allows control of the system temperature. A cooling system might be needed when the heat is generated too late during cycling to dissipate. Under non-uniform temperature distribution conditions, a cooling system is also needed to adjust the overall temperature manually. An optimal LIB operation range is 15–35 °C [126]. Thus, an optimal cooling control system capable of maintaining this range is essential for safe and prolonged battery service life and to reduce costs.

Depending on the method of heat transfer, typical battery thermal management systems include (1) traditional cooling systems (e.g., air-based systems with an electric fan), (2) liquid-based systems containing water, glycols, etc., (3) phase-change material (PCM)-based, and (4) heat pipe-based thermal management systems [127]. As outlined below, these systems all have advantages and disadvantages, as well as specific applications, but their pri-
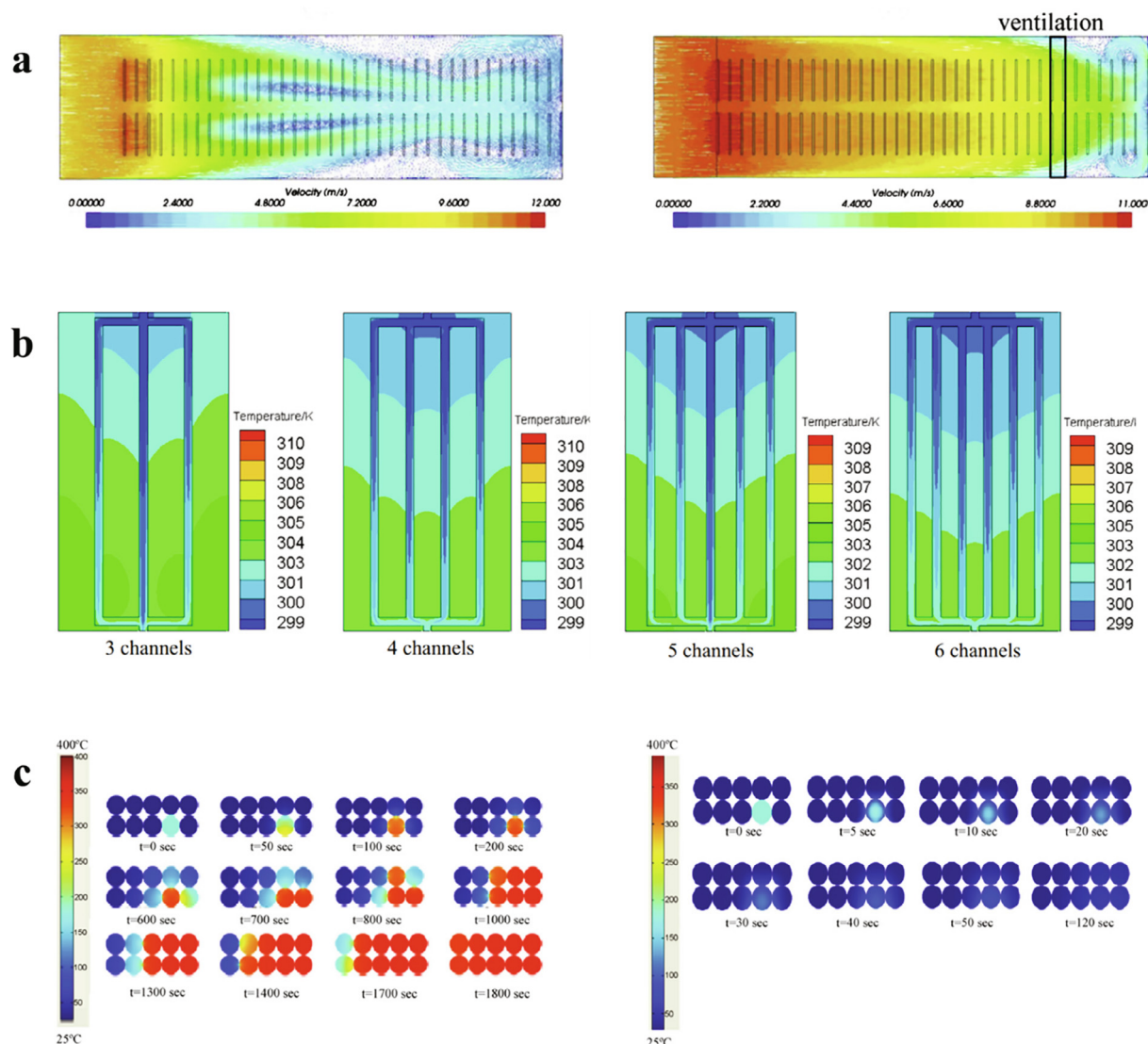
Fig. 6. (a) Top view of velocity and pressure distributions in an inlet manifold (left) with and (right) without ventilation of a LIB module. Copyright (2013) Elsevier [132]. (b) Temperature distribution under different cooling channels. Copyright (2016) Elsevier [133]. (c) Thermal runaway spreading triggered by one runaway cell in air-cooled module with (left) and without (right) PCM microencapsulation. Copyright (2009) Elsevier [138].

mary purposes are to control battery temperatures and minimize formation of localized hot spots.

Air cooling systems (i.e. systems that use air as a medium to remove heat) are structurally simple and easy to maintain. They are classified as either 'natural' or 'forced' cooling systems, depending on whether or not energy is specifically used to drive them. Natural cooling simply relies on the temperature difference between a battery and ambient air to cool the battery. If convection is insufficient to dissipate the internal heat of the battery at its maximal charge and discharge rates, a fan or a blower can be used to increase ('force') the movement of air around it and improve thermal exchange [128].

In liquid cooling systems, a liquid is used as a refrigerant to remove heat generated by a battery. Compared with air, liquids have greater thermal conductivity, thinner boundary layers and greater heat capacities [129]. Depending on whether the liquid is in contact with the battery, the system provides either direct or indirect liquid cooling. Immersion cooling cools all sides of the battery, thereby helping to improve temperature consistency. For safety reasons, however, such as potential short circuits and elec-

trochemical corrosion, immersion cooling is not currently used in EVs [130].

The coolant selected relates profoundly the entire cooling process, the battery structure and cell arrangement, the position of the liquid and air inlets/outlets, coolant flow rate. In the Tesla liquid cooling system a water and ethylene glycol mixture (in a 1:1 mass ratio) is used as a coolant, and the cooling pipes meander through the 18,650 stack of cells to improve heat dissipation efficiency [131]. Zhao et al. found that the performance of a fan-based air cooling system was best when the fan was positioned on top of the module (Fig. 6a), and a forced air cooling cubic arrangement provided the optimal combination of cooling effect and cost [132]. To enhance the cooling effect even more, optimization of the inter-cell distance in a battery module is generally recommended (Fig. 6b) [133]. Increasing the spacing between the cells and airflow rate can moderate temperature rises. However, while bigger channels improve cooling efficiency they result in uneven temperature distributions, and optimization of spacing improves temperature uniformity over a module. Ideally, the channel size should match the coolant's Reynolds number [134]. Cool-

ing of batteries with layout limitations is often uneven, so suitable gas or liquid flow paths must be designed. For example, in some designs, the vortices at the inlet manifold are suppressed by the ventilation hole geometry, but this effect can be used to obtain a more uniform flow velocity [135].

As the battery power density increases, raising the heat transfer coefficient becomes increasingly crucial. This can be done by applying mini-channels and enabling the cold plates to dissipate the heat effectively. Excellent cooling efficiency of such mini-channel cold-plate thermal management systems has been achieved during battery discharge at 5C rate. In fact, the five-channel design was sufficient [136]. Additional cooling (if needed) can be provided via increasing the inlet flow rate.

It involves selecting a PCM with a suitable melting temperature and using the heat it absorbs and releases during phase changes to cool and warm a battery when the temperature respectively rises above and falls below that temperature. As it relies on the transfer of phase-change heat and there is no external energy input, this involves a passive continuous circulation process. The thermal conductivity is small, 0.1 ~ 0.3 W/(m·K), and it is difficult to place a large amount of PCM in a limited space, so the heat exchange is limited, which can easily cause large temperature differences in the battery pack [137]. Thus, when used in battery thermal management, PCM must be combined with other cooling methods.

As an effective and elegant approach for compact battery forced air-cooling, PCM cooling allows for straightforward cooling designs. In modeling that was reported, under a simulated air-cooling system, battery thermal runaway could be triggered by even failure of a single individual cell upon internal short-circuit, which led to a local temperature increase up to 180 °C [138]. In sharp comparison, with the use of PCM-based cooling, thermal runaway did not occur and temperature of the module maintained within normal operational limits. A PCM-graphite matrix with high thermal conductivity was enabled to absorb and spread heat rapidly (Fig. 6c), but PCM cooling does not conduct heat from cell to cell as quickly as air cooling. To improve PCMs' low thermal conductivity, and thus exploitation of its greater heat storage capacity, researchers have proposed several possible solutions, including embedding metal-based materials [139], impregnating porous media [140] and combining them with fin structures to increase their thermal conductivity and mass [141]. Lin et al. used PCM to wrap batteries, with graphite sheets between the batteries to increase thermal conductivity, thereby enhancing the heat loss and significantly improving the uniformity of the battery pack temperature [142]. Zhang et al. used copper fiber as a skeleton and filled it with paraffin to form a coating material in tests showing that appropriate design can improve the heat transfer performance of the filling material and keep the maximum temperature difference of the battery pack used in the tests to within 5 ℃ [143]. Ping et al. proposed the addition of fins on the outer surface of the PCM to optimize the thermal management structure and enhance the thermal conductivity of a battery pack [144].

A direct cooling and heat management system uses the phase-change heat of a refrigerant to reduce the battery temperature effectively and improve the consistency of the battery pack temperature [145]. The coolant absorb additional and excessive heat from the battery surface to cool battery by evaporation. Unsimilar to the traditional liquid cooling, which requires non-cost-effective equipment, such as pumps, cold plates, and heat exchangers, evaporation is essentially an atmospheric process, so it requires minimal energy and operating costs.

4.2.2. Cell balance

It is difficult to produce totally identical battery cells, due to variations during the manufacturing and assembly processes, as well as surrounding environment. Thus, during battery operation,

even little differences between each single cell will intensify and accumulate if no measures are taken. In the absence of an appropriate balancing system, the voltage differences between the individual cells will amplify, severely compromising battery safety [146]. To achieve a high-performance battery system, the cells need to be continuously balanced for minimizing the variations between them [147].

Both external and internal factors can lead to cell imbalance. Internal factors include those related to variations in internal impedance, and stability of electrode interface with electrolyte. External factors are for those related to multi-rank pack protection integrated circuits. In addition, thermal differences in a battery can cause different self-discharge rates in its cell components [148].

Battery balancing typically involves measurement and comparison of the voltages, capacities or SOCs of all cells after each charging cycle and can be either passive or active [149]. Passive equalization technology is currently widely-used, but active equalization technology is becoming more and more popular and used in certain specific market segment.

Passive equalization involves use of energy-consuming components to convert excess power in a single cell into heat energy for consumption, thereby decreasing the inconsistency between cells (Fig. 7a and b). The main type of passive balancing is switch resistance, in which equalizing resistance of the access circuit consumes some of the battery energy through heat generation. Passive equalization can release the electrical energy of the overcharged high-capacity cells in the battery pack, but it cannot supplement the energy for the low-capacity cells. The circuit structure used in passive equalization systems is relatively simple and the energy-consuming components can be continuously discharged. Moreover, they can also be discharged in an intermittent manner, depending on the input signal [150]. During the battery charging process, the equalization control circuit monitors the voltage, SOC and other state parameters of all cells in the battery pack (Fig. 7d). By controlling the switch, the resistance is applied to discharge the high-power battery cell to consume energy, while the low-power cell switch is turned off, and no discharge energy is consumed, and finally equilibrium is achieved (Fig. 7e). Since the charging current of a single battery is automatically corrected according to its balance, as the charging progresses its voltage difference continuously declines, and a good balance is reached in later stages of the charging (Fig. 7f) [151].

Active equalization involves use of various kinds of circuit topologies and control strategies that non-dissipatively transfer energy between different batteries and modules, thereby equalizing the system (Fig. 7a and c). Active equalization is superior to passive equalization in terms of energy utilization and equalization efficiency. However, its application is currently limited by difficulties in developing small systems that are easy to integrate, cheap, fast, and reliable. Current active equalization strategies include several approaches based on capacitance, inductance, and transformers [152], which commonly adjust variables including actual voltage, battery capacity and SOC in the equalization process [153].

Dong and Han proposed a new architecture in which equalizers (including switching devices, gate drivers, inductors and digital signal processing controllers) are placed in parallel layers. All the equalizers can storage energy from high SOC cells and charge to low SOC cells (Fig. 7g). As a result, it takes less than one hour to have all the cells with 62%, 48%, 63%, and 42% SOCs have the same SOCs at the end of the experiment (Fig. 7h) [154].

5. LIB safety standards and tests

LIB safety standards and test methods are intended to be developed to ensure that LIBs and their components meet specified
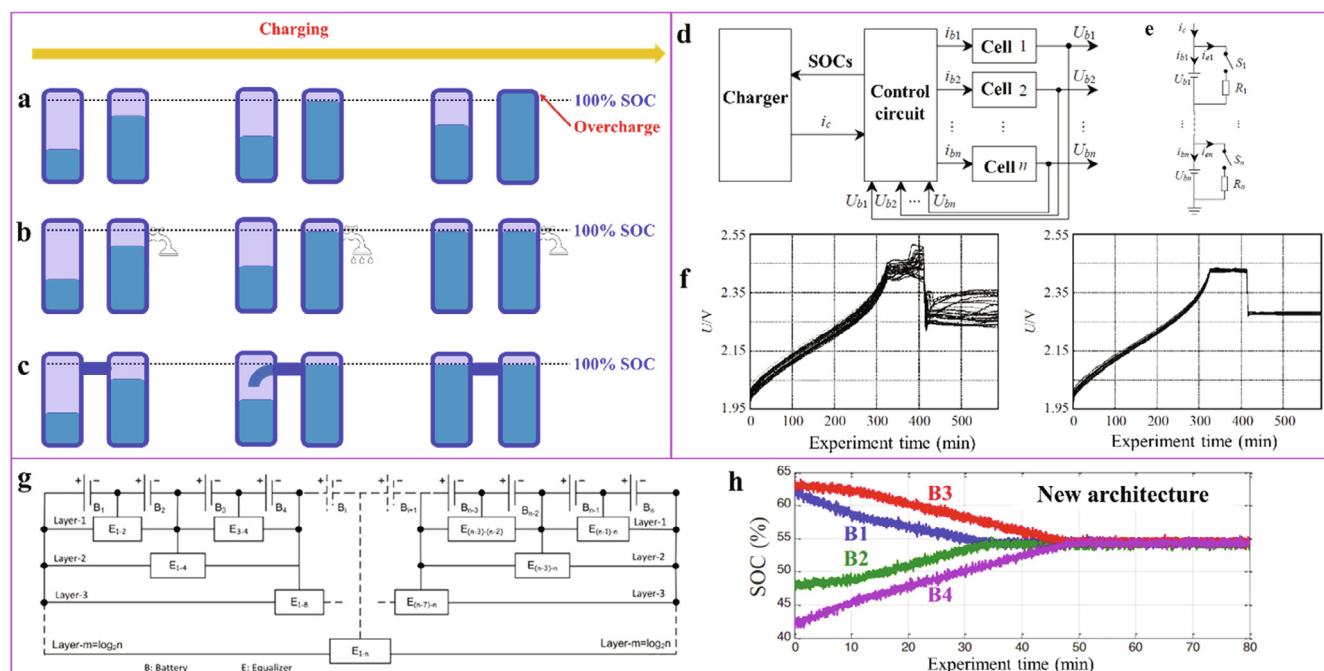
Fig. 7. Charging battery is similar to adding water in water tank. (a) Adding water with the same flow rate to two cells with different water contents, so the water tank with higher content will fill full firstly. Further adding water will spill over (overchare). (b) Further added water will be released to ground (passive equalization). (c) Further added water will be released to the other cell (active equalization). (d) Topological structure of battery equalization. (e) Battery equalization using resistor equalizing circuit. (f) Cell voltage without (left) and with (right) equalization circuit [151]. (g) Battery equalization architecture in which equalizers are placed in different nested layers. (h) Battery equalization results [154].

safety criteria, especially if they are produced commercially. Standardized settings and tests are essential for ensuring that batteries available on the market are of sufficient quality for intended purposes. Thus, these tests are as crucial for the future development of portable electronics and EVs as the LIBs themselves.

To reduce the thermal runaway risk in commercially available products, LIBs for vehicles should be certified in accordance with relevant safety testing standards before mass production or sale. Safety test standards are designed to ensure that certified LIBs have sufficiently low risks of safety accidents in specified kinds of thermal runaway induction and expansion situations.

Battery safety standards are constantly being updated and optimized, because current tests cannot fully guarantee their safety in practical applications. This is still a very serious problem, as there are fires in electric vehicles almost every week around the world. Hence, various international safety organizations regulate battery safety, and governments of different countries have formulated safety standards in accordance with national requirements and conditions and have gradually improved the safety standards of lithium-ion batteries. Academics and industrial groups have also carried out extensive research on battery safety.

5.1. Safety standards

Most countries and international organizations have developed LIB-safety oriented standards (Table 3), which include:

(1) Chinese standard GB/T 31,485 [155];
(2) Society of Automotive Engineers (SAE) standard 2464 [156];
(3) International Electrotechnical Commission (IEC) standard IEC62133 Edition 2.0 [157];
(4) United Nations (UN) standard UN38.3 [158];
(5) Japanese Industrial Standard (JIS) C8714 [159];

(6) Underwriters Laboratories (UL) standard UL2580 Edition 2.0 [160];
(7) International Standardization Organization (ISO) standard ISO 16750–2 [161].

The various safety test standards apply different methodologies, so we provide in Table 4 a summary of some test requirements and comparisons of five test items in the standards. The table shows that different standards have distinct and very specific test parameters [155-182], but with overlaps in their methodologies. For example, for the hot box experiment, three of the standards require 'hot box tests' of batteries at 130 °C.

The test standards are formulated to reduce the probability of thermal runaway accidents in actual use. Thus, they are intended to assess responses of batteries in real potential situations, with continuous updates and upgrades in accordance with the ongoing development of LIB technology, which reflects concerns about the causes and hazards of accidents that have occurred.

Overcharge/over-discharge tests are intended to assess overcharge/over-discharge processes that occur in a cell when the charge and discharge process is out of control. External short circuit tests assess the short circuiting that is caused by external electrical connections of battery poles under abnormal conditions. Drop tests assess responses of batteries to rigid impact during transportation and use. Heating tests assess the thermal runaway caused by a battery being heated due to local overheating, and the subsequent thermal runaway expansion. Crush tests assess responses of battery cells being mechanically deformed by an external force in a collision accident, resulting in separator rupture, cathode and anode connection, short circuiting, and eventually thermal runaway. Nail penetration tests assess effects of a battery short circuiting if the separator is penetrated by impurities. Temperature shock tests assess batteries' responses to extreme temperatures during operation.

Table 3
International safety test standards for LIBs intended for use in EVs.

Standard system	Standard code	Standard full name	Published year	Standards series	Application Scope	Technical characteristics
Freedom CAR	SAND 2005–3123 [162]	Electrical energy etorage system abuse test Manual for electric and hybrid electric vehicle applications	2006	SAND 99–0497 [163]	Battery cell, module and pack	Requirements for electrical performance, environmental suitability and safety performance
SAE	SAE J2464-2009 [156]	Electric and hybird vehicle rechargeable Energy storage system safety and abuse testing	Released in 1999, revised in 2009	SAE J1715 [164] SAE J1739 [165] SAE J1950 [166] SAE J2344 [167]	Battery pack and battery system	Security requirements
GB/T	GB/T 31485–2015 [155]	Safety requirements and test methods for traction battery of electric vehicles	2015	GB/T 31484–2015 [168] GB/T 31486–2015 [169] GB/T 31467.3–2015 [170]	Battery cell and module	Requirements for electrical performance, environmental suitability and safety performance
UN	UN38.3 [158]	United Nations manual on hazardous materials transport tests and standards, part 3, section 38.3	2015	-	Battery cell, module and pack	Security requirements
ISO	ISO 16750–2 [161]	Road vehicles - environmental conditions and testing for electrical and electronic equipment - part 2: electrical loads	2010	ISO 16750–1 [171] ISO 16750–3 [172] ISO 16750–4 [173] ISO 16750–5 [174]	Battery cell, module and pack	Reliability and safety test specifications
IEC	IEC 62660–2-2010 [175]	Secondary Lithium Ion Cells for the propulsion of electric road vehicles – part 2: reliability and abuse testing	2010	IEC 62660–3-2016 [175] IEC 60068–2-2 [176] IEC 62133–2012 [177]	Battery cell	Reliability and safety test specifications
UL	UL 2580–2010 [125]	Battery safety standards for electric vehicles	2013	UL 1642–2009 [178] UL 2054–2009 [179]	Battery cell, module, pack and system	Requirements for electrical performance, environmental suitability and safety
GM	GM-Modified USABC [180]	General motors battery test standard for electric vehicles	2016	-	Battery cell and module	Requirements for electrical performance and abuse tolerance
VW	VW PV8450 [181]	Volkswagen battery test standards for electric vehicles	2016	-	Battery cell, module and pack	Requirements for electrical performance and abuse test
SMTC	SMTC 9 N20 011–2018 [182]	Electrochemical performance test Specification of electric vehicles for lithium-ion battery	2018	-	Battery cell, module and pack	Requirements for electrical performance

5.2. Safety tests

LIB safety assessment involves a myriad of tests that a battery must pass to certify that it will not be hazardous under specified abuse conditions. Table 5 shows the main safety tests used to examine key LIB properties. Analysis of the presence of various LIB defects and shortcomings can help to define specific LIB safety issues or hazards. Extensive testing uncovers these issues to assist efforts to ensure that future generations of batteries are safer and more reliable. Table 5 shows electrochemical, mechanical, and thermal tests included in current standards to ensure the safety of LIBs before they enter the market.

In a safety test possible trigger modes are simplified so batteries' thermal runaway characteristics are measurable in the laboratory. Laboratory environment test conditions must generally be more stringent than 'real-world' conditions to ensure safety during actual use. For example, batteries being tested have to be maintained at a 100% SOC.

In addition to the actual cause of an accident, three principles should be met in the process of formulating a safety standard:

(1) Test operability: the safety test should be feasible, with no unscientific or technically incorrect elements.
(2) Repeatability of the test: all aspects of the test should be as similar as possible, and consistent results should be obtained in multiple tests of a given battery sample at the same test center, using the same experimental equipment, under the same conditions.

(3) Test reproducibility: similar results should be obtained when the test is conducted in different centers, with similar equipment and the same test conditions.

5.2.1. Overcharge tests

According to the IEC standard test, the cell is first discharged to 3.0 V at 0.2C rate, and then is charged under 10 V and an arbitrarily set current I within the time is equal to $2.5 \times \frac{c_5}{I}$. If the battery does not combust or explode during or after the test it is considered safe, its materials (electrolyte, active electrode materials, separators etc.) are regarded as having adequate properties, and the structural design is deemed satisfactory. The safety performance under overcharge is closely related to the charge rate, so overcharging is performed at different rates to establish at which extreme rate and voltage failure occurs. As various battery types are intended to have specific applications, batteries are typically tested using tests corresponding to specific applications and conditions [157].

5.2.2. Heating tests

Batteries swell and often explode at elevated temperatures, because their heat release rate is higher than their cooling rate, causing electrolyte decomposition and interfacial electrode–electrolyte reactions. Thus, as LIBs store large amounts of chemical energy, heating tests should be performed to examine their performance in high-temperature conditions.

Heating is used to analyze LIBs' thermal stability and heat distribution to ensure they have sufficiently efficient heat manage-

Table 4
Comparison of selected items in six safety testing standards.

Test content	Safety testing standard					
	GB/T31485 [155]	IEC62133 [157]	UL2580 [160]	SAE J2464 [156]	VW PV8450 [181]	USABC-GM [180]
Heating	Heating at 5 ℃/min from 25 ℃ to 130℃, hold for 30 mins	130 ℃, 10 mins	150 ± 2 ℃, 60 mins	Max. stable temperature	2 ℃/min to 130 ℃ or 200 ℃ hold for 30 mins	0.5 ℃/min, 50-150 ℃, hold for 30 mins
Short-circuit	Short circuit for 10 mins, $R{\leq}5$ mΩ	80±20 mΩ	Short with $R{\leq}5$ mΩ until explosion, fire or no temp change	$R{\leq}5$ mΩ for hard short; $R{\geq}5$ mΩ for soft short	short 10 mins, $R{\leq}1$ mΩ, $R = 5$ mΩ, R=10 mΩ	Short circuit for 10 mins, $R{\leq}5$ mΩ
Overcharge	100% SOC Overcharge to 1.5 V_{max} or charge for 1 hour at 1C	Overcharge to 250% SOC at 1C	Overcharge to 200% SOC at 1C	Overcharge to 200% SOC at 1C	Overcharge to 1.1 V_{max} or 5 mins at 1C	Overcharge the 100% SOC cell at 1C for 1 hour or 1.5 V_{max} or venting
Over-discharge	Over-discharge the 100% SOC cell at 1C for 1.5 hours	Over-discharge the 0% SOC cell at 1C for 90 mins	Over-discharge the 0% SOC cell at 1C for 90 mins	Over-discharge the cell to −100% SOC	/	Over-discharge the 100% SOC cell at 1C until venting
Nail penetration[1]	Penetration rate 25 mm/s, φ 5~ 8mm, 100% depth	/	80 mm/s, φ 3 mm, 100% depth	80 mm/s, φ 3 mm, 100% depth	0.1 mm/s, φ 1 mm stainless steel, 2 mm depth	80 mm/s, φ 3 mm, 100% depth

[1] φ represents the nail diameter.

Table 5
Current safety tests for LIBs before they enter the market.

Focal properties	Main tests
Electrochemistry performance	Overcharge and over-discharge, high- and low-temperature discharge, external short circuit, and forced discharge
Mechanical properties	Drop, heavy impact, nail penetration, shake and squeeze, acceleration, and crush
Thermal performance	Heating, thermal shock, and spark
Surroundings	Low pressure, high altitude, and soaking

Table 6
Standard test methods simulating LIB internal short-circuits.

Test methods	Standard number
Nail penetration	GB 31485–2015 [31]UL 2580:2016 [156]
Heavy impact	UN 38.3 [157]
	UL 2580:2016 [160]
Crush	IEC62133:2012 [156]
	UL 2580:2016 [160]
Forced internal short circuit	JIS C8714:2007 [159]

ment and capability to forecast potential hazards. The results are then used to assess how thermal abuse consequences can be alleviated. Specifically, data obtained from hot box experiments are used to simulate their thermal characteristics, and distributions of internal and external temperatures, then assess possible improvements in their design, materials, cooling systems, etc. Some electrochemical models also use thermal shock results to simulate electrochemical reactions and heat transfer as functions of the internal and external temperatures. According to the GB/T 31,485 heating procedure, a battery should be placed in a hot box, heated to 130 ± 2 ℃ at 5 ℃/min and kept at this temperature for 30 minutes. If the battery does not leak or combust during this thermal shock test, it is considered safe.

5.2.3. Short circuit tests
5.2.3.1. External short circuit tests.
A designed external short-circuit test is aimed to evaluate the LIB safety performance. According to the GB31485-2015 procedure, the battery is kept at 25 ± 2 ℃ in a fully charged state for 30 minutes, then the cathode and anode terminals are connected with a wire, and the external resistance is kept at 5 mΩ. During this test, the temperature and voltage are monitored simultaneously, throughout the entire test [31]. The test is considered successful if the cell does not explode or combust.

5.2.3.2. Internal short circuit tests.
High current passes through a short-circuited site, generating a large quantity of heat, which might casue thermal runaway. Thus, tests have been developed to assess battery performance under internal short-circuit conditions, and the International Electrotechnical Commission (IEC), Institute of Electrical and Electronics Engineers (IEEE), Underwriters Laboratories (UL), and other organizations have published reports on specific short-circuit simulation methods (see Table 6).

5.2.3.3. Nail penetration tests.
These tests are designed to simulate internal battery short circuits that may occur when a battery's internal membrane is penetrated by impurities. According to GB/T 31485, a fully-charged battery should be penetrated with a high temperature-resistant steel spike of φ 5 ~ 8 mm (with a conical spike tip angle of 45 ~ 60°, and surface that is clean, smooth, and free of rust, oxidized layer and dirt) in a direction perpendicular to the polar plate at a speed of 25 ± 5 mm/s. The penetration position should also be close to the geometric center of the penetrated surface, with the steel spike retained inside the battery. The test is considered successful if the cell does not explode or combust.

5.2.3.4. Crush tests.
During a crush test, a battery is mechanically compressed. According to GB/T 31485, the cells are first charged at 1C rate to 4.2 V, then the battery is placed between two planes in a semi-cylinder with a 75 mm radius, and subjected to crushing at 5 mm/s, with a load applied in the direction perpendicular to the battery's polar plate. The crushing is ceased when the voltage reaches 0 V, the deformation reaches 30%, or the crushing load reaches 200 kN. The test has a positive outcome if no fire or explosion is observed.

5.3. Hazard level

In evaluations of batteries' safety condition based on results of the above abuse tests, the EUCAR and SAE-J Hazard Levels and the associated criteria that are widely applied.

Typically, hazard levels of Electrical Energy Storage System (EESS) devices according to their responses to abuse conditions are assigned by EUCAR and presented in Table 7 [162]. Manufacturers and integrators may find it helpful and useful to take these levels into consideration when evaluating a given EESS design's abuse response.

Table 7
EUCAR hazard level and descriptions.

Hazard level	Description	Classification criteria and effects
0	No effect	No effect, no loss of functionality
1	Passive protection activated	No defect, no leakage, no venting, fire, or flame, no passive protection rupture, no explosion, no exothermic reaction or thermally activated runaway. Cell reversibly damaged. Repair of protection device needed.
2	Defect/damage	No leakage, no venting, fire, or flame, no rupture, no explosion, no exothermic reaction or thermal runaway. Cell irreversibly damaged. Repair needed.
3	Leakage Δmass < 50%	No venting, fire, or flame, no rupture, no explosion. Weight loss < 50% of electrolyte weight (electrolyte = solvent + salt)
4	Venting Δmass > 50%	No fire or flame, no rupture, no explosion. Weight loss > 50% of electrolyte weight (electrolyte = solvent + salt)
5	Fire or flame	No rupture, no explosion (i.e., no flying parts)
6	Rupture	No explosion, but flying parts of the active mass
7	Explosion	Explosion (i.e., disintegration of the cell)

Table 8
Hazard severity levels and descriptions (adapted from EUCAR and SAND 2005–3123).

Hazard severity level	Description	Classification criteria and effects
0	No effect	No effect, no loss of functionality.
1	Passive protection activated	No damage or hazard, reversible loss of function. Replacement or re-setting of protection device is sufficient to restore normal functionality.
2	Defect/damage	No hazard but damage to RESS. Irreversible loss of function. Replacement or repair needed.
3	Minor Leakage/ venting	Evidence of cell leakage or venting with RESS weight loss < 50% of electrolyte weight
4	Major Leakage/ Venting	Evidence of cell leakage or venting with RESS weight loss > 50% of electrolyte weight
5	Rupture	Loss of mechanical integrity of the RESS container, resulting in release of contents. The kinetic energy of released materials is not sufficient to cause physical damage external to the RESS.
6	Fire or Flame	Ignition and sustained combustion of flammable gas or liquid for more than approximately one second. Sparks are not flames.
7	Explosion	Very fast release of energy sufficient to cause pressure waves and/or projectiles that may cause considerable structural and/or bodily damage, depending on the size of the RESS. The kinetic energy of flying debris from the RESS may also be sufficient to cause damage.

The SAE recommends that results of each test should be reported in terms of the Hazard Severity levels described in Table 8 [156], and the use of such information in Battery safety and Hazard risk migration approaches. Rechargeable Energy Storage System (RESS) responses in abusive tests should be determined.

6. Summary

Broader application of LIBs is limited because safety concerns regarding their performance have not been fully addressed. Com-

prehensive analysis of their failure mechanisms in extreme conditions—such as over-(dis)charge, external short circuit, thermal, and mechanical abuse—has shown that LIB thermal runaway and the presence of flammable components are root causes of battery fires and explosions. A series of effective strategies have been developed based on knowledge obtained regarding LIB structures and working principles. LIB safety and performance stability can be significantly improved by carefully choosing electrode materials, separators, and electrolytes, and by optimizing battery design. External strategies, such as cooling and cell balancing, can also make significant contributions to LIB safety performance under normal conditions.

Various LIB safety standards and corresponding test programs have been developed, as reviewed in the preceding text. The main goal of these programs is to provide references for battery safety and standard ways to assess their performance under abnormal conditions, thereby facilitating improvements in predictions of battery performance and alleviation of the detrimental processes of thermal runaway and various kinds of abuse that increase risks of real-life accidents.

The following strategies are proposed for enhancing LIB safety, both externally and internally (Fig. 8).

The most effective way to dissipate excessive heat is to protect batteries from thermal and mechanical abuse by improving their outer shells. This is becoming increasingly important as the number of EVs on our roads is increasing, so there are correspondingly urgent needs to enhance LIB safety. There are also growing energy density requirements and demands for more powerful EV battery systems, which will generate even more heat and pose even greater thermal management challenges. The main strategies to meet these challenges focus on increasing the speed and uniformity of heat transfer in large, high-density batteries. However, increasing the mechanical reinforcement of LIBs to enhance their protection is also important, for example, adjusting outer casing materials to increase their impact resistance. Another solution would be to install batteries in parts of cars that are least affected during collisions and accidents. Thermal shock can also severely compromise LIB safety, and an electric car fire can cause other nearby vehicles to catch fire, but LIB thermal shock tolerance can be enhanced by various external measures and design strategies to decrease accidents when thermal shock occurs.

Heat generation and accumulation inside batteries are the main causes of LIB safety accidents. Heat generation is often accompanied by gas formation, and both processes are controlled by the battery voltage and temperature. Overcharge is one of the leading causes of heat generation. Thus, incorporating preventative measures to avoid spontaneous overcharging inside batteries would complement the external overcharge protection measures. Thermal runaway is caused by a battery short-circuiting due to separator failure and the inability of the localized heat to dissipate efficiently and quickly. The development of temperature-sensitive materials to use inside batteries to prevent localized temperature increases offers an excellent solution to the thermal runaway problem. Another promising heat dissipation approach is to provide internal pathways for rapid heat diffusion (for example, by incorporating materials with high thermal conductivity). Last, but not least, careful selection of active electrode materials and electrolytes is also essential for reducing heat and gas production, and to protect the electrode interfaces.

Successfully passing the nail penetration, crash, and other tests does not guarantee a car battery's safety in real-life performance conditions. Improvements to the manufacturing process and the development of new evaluation and test methods are therefore crucial for developing future generations of LIBs.
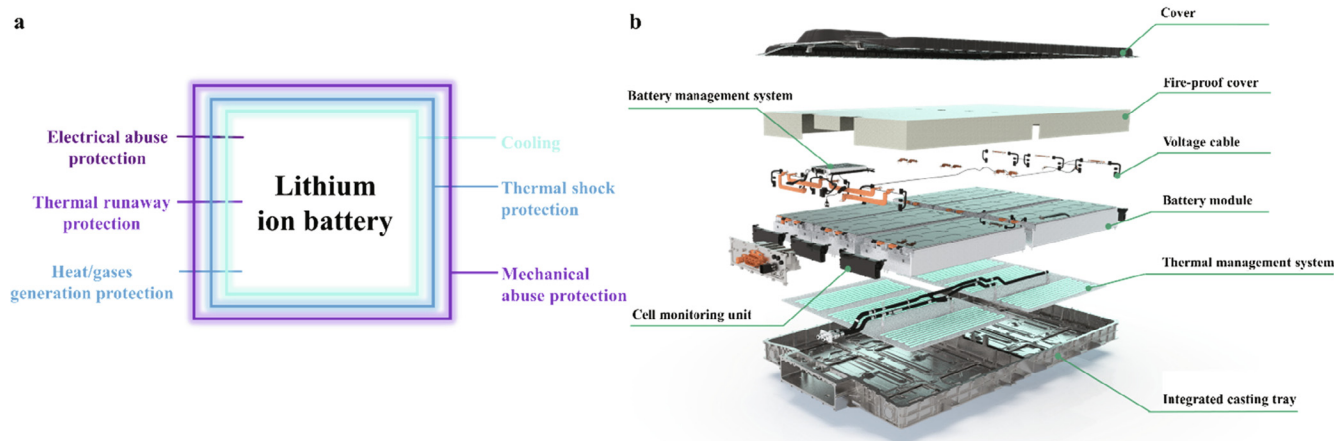
Fig. 8. (a) Strategies to improve lithium ion batteries' safety. (b) Schematic diagram of advanced battery pack in the car of ROEWE R ER6.

Declaration of competing interest

The authors declare that they have no known competing financial interests or personal relationships that could have appeared to influence the work reported in this paper.

Acknowledgments

References

[1] E. George, Blomgren, J. Electrochem. Soc. 164 (2017) 5019–5025.
[2] Y.S. Duh, K.H. Lin, C.S. Kao, J. Therm. Anal. Calorim. 132 (2018) 1677–1692.
[3] N.E. Galushkin, N.N. Yazvinskaya, D.N. Galushkin, J. Electrochem. Soc. 165 (2018) 1303–1308.
[4] Y. Kang, C. Deng, Y. Chen, X. Liu, Z. Liang, T. Li, Q. Hu, Y. Zhao, Nanoscale Research Lett. 15 (2020) 112.
[5] J. Yang, X. Liu, J. Tian, X. Ma, B. Wang, W. Li, RSC Adv. 7 (2017) 21061–21067.
[6] Y. Wang, C. Liu, R. Pan, Z. Chen, Energy. 121 (2017) 739–750.
[7] C.T. Love, C. Buesser, M.D. Johannes, K.E. Swider-Lyons, J. Electrochem. Energy. 15 (2018) 011006.
[8] D.P. Finegan, E. Darcy, M. Keyser, B. Tjaden, T.M.M. Heenan, R. Jervis, Adv. Sci. 5 (2017) 1700369.
[9] B. Liu, J. Zhang, C. Zhang, Eng. Fail. Anal. 91 (2018) 315–326.
[10] F. Schipper, E.M. Erickson, C. Erk, J.Y. Shin, F.F. Chesneau, D.J. Aurbach, J. Electrochem. Soc. 164 (2017) 6220–6228.
[11] X. Feng, M. Ouyang, X. Liu, Energy Storage Mater. 10 (2018) 246–267.
[12] X. Feng, M. Ouyang, X. Liu, J. Electrochem. Power sources. (2018).
[13] Z. Chen, R. Xiong, J. Lu, X. Li, Appl. Energy. 213 (2018) 375–383.
[14] D.P. Finegan, M. Scheel, J.B. Robinson, B. Tjaden, I. Hunt, T.J. Mason, Nat. Commun. 6 (2015) 6924.
[15] P. Huang, Q. Wang, K. Li, Sci. Rep. 5 (2015) 7788.
[16] P.G. Balakrishnan, R. Ramesh, T. Prem Kumar, J. Power Sources. 155 (2006) 401–414.
[17] N. Williard, W. He, C. Hendricks, M. Pecht, Energies. 6 (2013) 4682–4695.
[18] M. Ichimura, IEEE. 29th International Telecommunications Energy Conference. 978 (2007) 687–692.
[19] The Sunday Mail, S. Aust Adelaide (Eds.), Laptop battery recall widens: 1, State Edition., News Limited, 2006.
[20] Q. Zhao, Z. Guo, Y. Wu, L. Wang, Z. Han, X. Ma, Y. Zhu, C. Cao, Sci. China Mater. 62 (2019) 1385–1392.
[21] X. Chen, H. Li, Z. Yan, F. Cheng, J. Chen, Sci. China Mater. 62 (2019) 1515–1536.
[22] Y. Cai, L. Ku, L. Wang, Y. Ma, H. Zheng, W. Xu, J. Han, B. Qu, Y. Chen, Q. Xie, D.L. Peng, Sci. China Mater. 62 (2019) 1374–1384.
[23] L. Wang, S. Yin, Z. Yu, Y. Wang, T.X. Yu, J. Zhao, Mater. Des. 160 (2018) 601–610.
[24] D. Miranda, C.M. Costa, A.M. Almeida, S. Lanceros-Mendez, Appl. Energy. 165 (2016) 318–328.
[25] Y. Kang, C. Deng, X. Liu, Z. Liang, T. Li, Q. Hu, Y. Zhao, Nanoscale Research Lett. 15 (2020) 147.
[26] B. Liu, Y. Jia, J. Li, S. Yin, C. Yuan, Z. Hu, J. Mater. Chem. A. 6 (2018) 21475–21484.
[27] S. Koch, F. Alexander, K.P. Birke, J. Power Sources. 398 (2018) 106–112.
[28] F. Larsson, P. Andersson, B.E. Mellander Blomqvist, Sci. Rep. 7 (2017) 10018.
[29] F. Larsson, S. Bertilsson, M. Furlani, J. Power Sources. 373 (2018) 220–231.
[30] A.W. Golubkov, S. Scheikl, R. Planteu, G. Voitic, H. Wiltsche, C. Stangl, G. Fauler, A. Thaler, V. Hacker, RSC Adv. 5 (2015) 57171–57186.
[31] AQSIQ, SAC. Safety requirements and test methods for traction battery of electric vehicles. 2015
[32] J. Duan, X. Tang, H. Dai, Y. Yang, W. Wu, X. Wei, Y. Huang, Electrochemical Energy Reviews 3 (2020) 1–42.
[33] K. Liu, Y. Liu, D. Lin, A. Pei, Y. Cui, Science Advances. 4 (2018) eaas9820.
[34] D.H. Doughty, E.P. Roth, Electrochemical Society Interface. 21 (2012) 37.
[35] X. Feng, D. Ren, X. He, M. Ouyang, Joule. 4 (2020) 743–770.
[36] B. Dunn, H. Kamath, J.M. Tarascon, Science. 334 (2011) 928–935.
[37] Y. Kang, Z. Liang, Y. Zhao, H. Xu, K. Qian, X. He, T. Li, J. Li, Sci. China Mater. 63 (2020), https://doi.org/10.1007/s40843-020-1327-8.
[38] X. Liu, D.S. Ren, H. Hsu, X. Feng, G.L. Xu, H. Gao, C. Lu, X. Han, Z. Chu, J. Li, X. He, K. Amine, M. Ouyang, Joule. 2 (2018) 2047–2064.
[39] W. Lu, I. Belharouak, J. Liu, K. Amine, J. Power Sources. 174 (2007) 673–677.
[40] K. Amine, I. Belharouak, Z. Chen, T. Tran, H. Yumoto, N. Ota, S.T. Myung, Y.K. Sun, Adv. Mater. 22 (2010) 3052–3057.
[41] J.M. Tarascon, M. Armand, Nature. 414 (2001) 359–367.
[42] Y. Inui, Y. Kobayashi, Y. Watanabe, Y. Watase, Y. Kitamura, Energy Conv. Manag. 48 (2007) 2103–2109.
[43] T. Wierzbicki, E. Sahraei, J. Power Sources. 241 (2013) 467–476.
[44] Z.Y. Jiang, Z.G. Qu, J.F. Zhang, Z.H. Rao, Appl. Energy. 268 (2020) 115007.
[45] M. Winter, B. Barnett, K. Xu, Chem. Rev. 118 (2018) 11433–11456.
[46] Q. Wang, P. Ping, X. Zhao, G. Chu, J. Sun, C. Chen, J. Power Sources. 208 (2012) 210–224.
[47] G. Guo, B. Long, B. Cheng, S. Zhou, P. Xu, B. Cao, J. Power Sources. 195 (2010) 2393–2398.
[48] G.H. Kim, A. Pesaran, R. Spotnitz, J. Power Sources. 170 (2007) 476–489.
[49] J. Lamb, C.J. Orendorff, J. Power Sources. 247 (2014) 189–196.
[50] H. Maleki, G. Deng, A. Anani, J. Howard, J. Electrochem. Soc. 146 (1999) 3224–3229.
[51] A. Randolph, Leising, J. Marcus, Palazzo, E.S. Takeuchi, J. Kenneth, Takeuchi, J. Power Sources. 97 (2001) 681-683.
[52] P. Donal, Finegan, M. Scheel, B. James, Robinson, B. Tjaden, M.D. Michiel, G. Hinds, J. L. Dan, Brett, R. Paul, Shearing, Chem. Phys. 18 (2016) 30912-30919.
[53] R. Jung, M. Metzger, F. Maglia, C. Stinner, A. Hubert, Gasteiger, J. Electrochem. Soc. 164 (2017) 1361–1377.
[54] J. Wang, Z. Hu, X. Yin, Y. Li, H. Huo, J. Zhou, L. Li, Electrochimi Acta. 159 (2015) 61–65.
[55] D. Ren, X. Feng, L. Lu, M. Ouyang, S. Zheng, J. Li, X. He, J. Power Sources. 364 (2017) 328–340.
[56] S.H. Kim, K.H. Choi, S.J. Cho, J.S. Park, K.Y. Cho, C.K. Lee, S.B. Lee, J.K. Shim, S.Y. Lee, J. Mater. Chem. A. 2 (2014) 10854–10861.
[57] B. Liu, Y. Jia, C. Yuan, L. Wang, X. Gao, S. Yin, J. Xu, Energy Storage Mater. 24 (2020) 85–112.
[58] Y. Chen, J.W. Evans, J. Electrochem. Soc. 143 (1996) 2708–2712.

[59] E. Sahraei, J. Meier, T. Wierzbicki, J. Power Sources. 247 (2014) 503–516.
[60] X. Zhang, T. Wierzbicki, J. Power Sources. 280 (2015) 47–56.
[61] C. Zhang, J. Xu, L. Cao, Z. Wu, S. Santhanagopalan, J. Power Sources. 357 (2017) 126–137.
[62] D.P. Finegan, M. Scheel, J.B. Robinson, B. Tjaden, I. Hunt, T.J. Mason, D.J. Brett, Nat. Commun. 6 (2015) 6924.
[63] L. Greve, C. Fehrenbach, J. Power Sources. 214 (2012) 377–385.
[64] M.Y. Ali, W.J. Lai, J. Pan, J. Power Sources. 242 (2013) 325–340.
[65] Y. Xia, T. Li, F. Ren, Y. Gao, H. Wang, J. Power Sources. 265 (2014) 356–362.
[66] R. Zhao, J. Liu, J. Gu, Appl. Energy. 173 (2016) 29–39.
[67] X. Li, K. Qian, Y.B. He, C. Liu, D. An, Y. Li, D. Zhou, Z. Lin, B. Li, Q.H. Yang, F. Kang, J. Mater. Chem. A. 5 (2017) 18888–18895.
[68] W. Zhao, G. Luo, C.Y. Wang, J. Electrochem. Soc. 162 (2015) A207–A217.
[69] C.H. Doh, D.H. Kim, H.S. Kim, H.M. Shin, Y.D. Jeong, S.I. Moon, B.S. Jin, S.W. Eom, H.S. Kim, K.W. Kim, D.H. Oh, A. Veluchamy, J. Power Sources. 175 (2008) 881–885.
[70] S. S. Zhang, J. Power Sources. 162 (2) 1379-1394.
[71] T. AOhsaki, T. Kishi, T.Kuboki, N. Takami, N. Shimura, Y. Sato, A. Satoh, J. Power Sources. 146 (2005) 97-100.
[72] J. Arai, Y.Okada, T.Sugiyama, M. Izuka, K. Gotoh, K. akeda, J. Electrochem. Soc. 162 (2015) 952-958
[73] D. Lisbona, T. Snee, Process Saf. Environ. Protect. 89 (2011) 434–442.
[74] H. F., Li, J.K. Gao, S.L. Zhang, Chinese J. Chem. 26 (2008) 1585-1588.
[75] D. Ouyang, M. Chen, J. Liu, R. Wei, J. Weng, J. Wang, RSC Adv. 8 (2018) 33414–33424.
[76] R. Guo, L. Lu, M. Ouyang, X. Feng, Sci. Rep. 6 (2016) 30248.
[77] K. Qian, Y. Li, Y.B. He, D. Liu, Y. Zheng, D. Luo, B. Li, F. Kang, RSC Adv. 6 (2016) 30474–30483.
[78] F. Larsson, B.E. Mellander, J. Electrochem. Soc. 161 (2014) 1611–1617.
[79] A. Kriston, A. Pfrang, H. Döring, B. Fritsch, V. Ruiz, I. Adanouj, T. Kosmidou, J. Ungeheuer, L. Boon-Brett, J. Power Sources. 361 (2017) 170–181.
[80] Z. Wang, H. Yang, Y. Li, G. Wang, J. Wang, J. Hazard. Mater. 379 (2019) 120730.
[81] P. Liu, C. Liu, K. Yang, M. Zhang, F. Gao, B. Mao, H. Li, Q. Duan, Q. Wang, J. Energy Storage. 31 (2020) 101714.
[82] T.M. Bandhauer, S. Garimella, T.F. Fuller, J. Electrochem. Soc. 158 (2011) 1–25.
[83] Z. Zhang, D. Fouchard, J.R. Rea, J. Power Sources. 70 (1998) 16–20.
[84] M.N. Richard, J.R. Dahn, J. Electrochem. Soc. 146 (1999) 2068–2077.
[85] N.-S. Choi, I.A. Profatilova, S.-S. Kim, E.-H. Song, Thermochimica Acta. 480 (2008) 10–14.
[86] D.D. MacNeil, J.R. Dahn, The Journal of Physical Chemistry A. 105 (2001) 4430–4439.
[87] H.S. Kim, K. Kim, S.I. Moon, I.J. Kim, H.B. Gu, Journal of the Solid State, Electrochemistry. 12 (2008) 867–872.
[88] H. Jeong, J. Kim, J. Soon, S. Chae, S. Hwang, J.H. Ryu, S.M. Oh, Electrochimica Acta. 277 (2018) 59–66.
[89] R. Jung, M. Metzger, F. Maglia, C. Stinner, H.A. Gasteiger, J. Electrochem. Soc. 164 (2017) A1361–A1377.
[90] S.E. Sloop, J.K. Pugh, S. Wang, J.B. Kerr, K. Kinoshita, Electrochemical and Solid-State Letters. 4 (2001) A42–A44.
[91] H. Li, F. Wang, C. Zhang, We. Ji, J. Qian, Y. Cao, H. Yang, X. Ai, Energy Storage Mater. 17 (2019) 275-283
[92] Z. Liang, Y. Zhao, Y. Li, Energies. 12 (2019) 3391.
[93] E. Hu, X. Yu, R. Lin, X. Bi, J. Lu, S. Bak, K.W. Nam, H.L. Xin, C. Jaye, A. Daniel, K. Fischer, X.Q. Amine, Nature Yang, Energy. 3 (2018) 690–698.
[94] L. X. Yuan, Z. H. Wang, W. X. Zhang, X. L. Hu, J. T. Chen, Y. H., Huang, J. B. Goodenough, Energy Environ. Sci. 4 (2011) 269-284.
[95] P. J. Bugrynieca, N. Jonathan, Davidsonb, J. Denis, Cumminga, S. F. Brown, J. Power Sources. 414 (2019) 557-568.
[96] Y. Yu, J. Wang, P. Zhang, J. Zhao, J. Energy Storage. 12 (2017) 37–44.
[97] Y.K. Sun, M.J. Lee, C.S. Yoon, J. Hassoun, K. Amine, B. Scrosati, Adv. Mater. 24 (2012) 1192–1196.
[98] The data is from the lecture: https://www.bilibili.com/video/av668313076.
[99] J. Li, Z.F. Ma, Chem. 5 (2019) 3–6.
[100] H. Gao, F. Maglia, P. Lamp, K. Amine, Z. Chen, A.C.S. Appl. Mater. Interfaces. 9 (2017) 44542–44549.
[101] L. Zhu, T.-F. Yan, D. Jia, Y. Wang, Q. Wu, H.-T. Gu, Y.-M. Wu, W.-P. Tang, J. Electrochem. Soc. 166 (2019) A5437–A5444.
[102] P. Hou, F. Li, Y. Sun, M. Pan, X. Wang, M. Shao, X. Xu, ACS Sustainable Chem. Eng. 6 (2018) 5653–5661.
[103] Z.D. Li, Y.C. Zhang, H.F. Xiang, X.H. Ma, Q.F. Yuan, Q.S. Wang, C.H. Chen, J. Power Sources 240 (2013) 471–475.
[104] B. Xiong, R. Chen, F. Zeng, J. Kang, Y. Men, J. Membr. Sci. 545 (2018) 213–220.
[105] C. Shi, P. Zhang, S. Huang, X. He, P. Yang, D. Wu, D. Sun, J. Zhao, J. Power Sources. 298 (2015) 158–165.
[106] D. Li, D. Shi, Z. Yuan, K. Feng, H. Zhang, X. Li, J. Membr. Sci. 542 (2017) 1–7.
[107] X. Jiang, L. Xiao, X. Ai, H. Yang, Y. Cao, J. Mater. Chem. A. 5 (2017) 23238–23242.
[108] D.V. Carvalho, N. Loeffler, G.-T. Kim, S. Passerini, Membranes. 5 (2015) 632–645.
[109] J. Dai, C. Shi, C. Li, X. Shen, L. Peng, D. Wu, D. Sun, P. Zhang, J. Zhao, Energy Environ. Sci. 9 (2016) 3252–3261.
[110] K. Xiao, Y.Y. Zhai, J.Y. Yu, B. Ding, RSC Adv. 5 (2015) 55478–55485.
[111] H. Xiang, J. Chen, Z. Li, H. Wang, J. Power Sources. 196 (2011) 8651–8655.
[112] B. Zhao, R. Ran, M. Liu, Z. Shao, Materials Science and Engineering: R: Reports. 98 (2015) 1–71.
[113] Y. Sun, N. Liu, Y. Cui, Nature Energy. 1 (2016) 16071.
[114] Y. Sun, L. Wang, Y. Li, Y. Li, H.R. Lee, A. Pei, X. He, Y. Cui, Joule. 3 (2019) 1080–1093.
[115] C.K. Chan, H. Peng, G. Liu, K. McIlwrath, X.F. Zhang, R.A. Huggins, Y. Cui, Nature nanotechnology 3 (2008) 31–35.
[116] Z. Zeng, B. Wu, L. Xiao, X. Jiang, Y. Chen, X. Ai, Y. Cao, J. Power Sources. 279 (2015) 6–12.
[117] L. Jiang, Q. Wang, K. Li, P. Ping, L. Jiang, J. Sun, Sustain, Energy Fuels. 2 (2018) 1323–1331.
[118] Q. Wang, B. Mao, S.I. Stoliarov, J. Sun, Progress in Energy and Combustion Science. 73 (2019) 95–131.
[119] R. Chen, A.M. Nolan, J. Lu, J. Wang, X. Yu, Y. Mo, L. Chen, X. Huang, H. Li, Joule. 4 (2020) 812–821.
[120] L.P. Hou, H. Yuan, C.Z. Zhao, L. Xu, G.L. Zhu, H.X. Nan, X.-B. Cheng, Q.-B. Liu, C.-X. He, J.-Q. Huang, Q. Zhang, Energy Storage Materials. 25 (2020) 436–442.
[121] Y. Zhou, F. Zhang, P. He, Y. Zhang, Y. Sun, J. Xu, J. Hu, H. Zhang, X. Wu, J. Energy Chem. 46 (2020) 87–93.
[122] J. Gao, Q. Shao, J. Chen, J. Energy Chem. 46 (2020) 237–247.
[123] R. Xu, C. Yan, Y. Xiao, M. Zhao, H. Yuan, J.-Q. Huang, Energy Storage Materials. 28 (2020) 401–406.
[124] Z. Hou, J. Zhang, W. Wang, Q. Chen, B. Li, C. Li, J. Energy Chem. 45 (2020) 7–17.
[125] R. Chen, Q. Li, X. Yu, L. Chen, H. Li, Chem. Rev. 120 (2020) 6820–6877.
[126] W. Wu, S. Wang, W. Wu, K. Chen, S. Hong, Y. Lai, Energy Conv. Manag. 182 (2019) 262–281.
[127] D. Chen, J. Jiang, G.H. Kim, C. Yang, A. Pesaran, Appl. Therm. Eng. 94 (2016) 846–854.
[128] R. Zhao, S. Zhang, J. Liu, J. Gu, J. Power Sources. 299 (2015) 557–577.
[129] Y. Chen, J.W. Evans, J. Electrochem. Soc. 140 (1993) 1833–1838.
[130] F. Cai, S. Xu, G. Chang, J. Power Sources. 36 (2012) 1410–1413.
[131] D. Dan, C. Yao, Y. Zhang, Y. Qian, W. Zhuge, Chin. Sci. Bull. 64 (2019) 682–693.
[132] T. Wang, K.J. Tseng, J. Zhao, Z. Wei, Appl. Energy. 134 (2014) 229–238.
[133] T. Wang, K.J. Tseng, J. Zhao, Z. Wei, J. Power Sources. 238 (2013) 301–312.
[134] J. Xun, R. Liu, K. Jiao, J. Power Sources. 233 (2013) 47–61.
[135] H. Park, J. Power Sources. 239 (2013) 30–36.
[136] Z. Qian, Y. Li, Z. Rao, Energy Conv. Manag. 126 (2016) 622–631.
[137] Q. Wang, B. Jiang, B. Li, Y. Yan, Renew. Sust. Energ. Rev. 64 (2016) 106–128.
[138] R. Kizilel, R. Sabbah, J.R. Selman, S. Al-Hallaj, J. Power Sources. 194 (2009) 1105–1112.
[139] A. Hussain, I.H. Abidi, C.Y. Tso, K.C. Chan, Z. Luo, C.Y.H. Chao, Int. J. Therm. Sci. 124 (2018) 23–35.
[140] W.Q. Li, Z.G. Qu, Y.L. He, W.Q. Tao, Appl. Therm. Eng. 37 (2012) 1–9.
[141] M. Akgun, O. Aydın, K. Kaygusuz, Appl. Therm. Eng. 28 (2007) 405–413.
[142] C. Lin, S. Xu, G. Chang, J. Liu, J. Power Sources. 275 (2015) 742–749.
[143] M. Pan, Y. Zhong, Int. J. Heat Mass Transf. 126 (2018) 531–543.
[144] P. Ping, R. Peng, D. Kong, G. Chen, J. Wen, Energy Conv. Manag. 176 (2018) 131–146.
[145] Q. Huang, X. Li, G. Zhang, J. Zhang, F. He, Yang Li, Appl. Therm. Eng. 141 (2018) 1092–1100.
[146] B. Duan, Z. Li, P. Gu, Z. Zhou, C. Zhang, J. Energy Storage. 16 (2018) 160–166.
[147] M. Daowd, M. Antoine, N. Omar, P. Lataire, P. Van Den Bossche, V. Mierlo, Energies. 7 (2014) 2897–2937.
[148] L. Lu, X. Han, J. Li, J. Hua, M. Ouyan, J. Power Sources. 226 (2013) 272–288.
[149] J. Cao, N. Schofield, A. Emadi, IEEE Vehicle Power and Propulsion Conference, Harbin 2008 (2008) 1–6, https://doi.org/10.1109/VPPC.2008.4677669.
[150] Z.B. Omariba, L. Zhang, D. Sun, IEEE Access. 7 (2019) 129335–129352.
[151] S. Xu, J. Wang, J. Xu, Proceedings of the CSEE. 32 (2012) 43–48.
[152] M. Evzelman, M.M.U. Rehman, K. Hathaway, R. Zane, D. Costinett, D. Maksimovic, IEEE Trans. Power Electron. 31 (2015) 7887–7895.
[153] S.W. Moore, P.J. Schneider, SAE Technical Paper. No. (2001–01-0959.).
[154] B. Dong, Y. Han, IEEE Energy Conversion Congress and Exposition. 2011 (2011) 928–934.
[155] Z. Zhang, L. Zhang, L. Hu, C. Huang, Int. J. Energy Res. 44 (2020) 2535–2548.
[156] SAE, J2464. Electric Vehicle Battery Abuse, Testing. (1999).
[157] IEC 62133. Secondary cells and batteries containing alkaline or other non-acid electrolytes-Safety requirements for portable sealed secondary cells, and for batteries made from them, for use in portable applications. 2012.
[158] , Transport of Dangerous Goods. (2015).
[159] JIS C 8714. Safety tests for portable lithium ion secondary cells and batteries for use in portable electronic applications. 2007.
[160] UL2580. Standard for Safety Batteries for Use in Electric Vehicles. 2016.
[161] ISO, 16750–2. Road vehicles-Environmental conditions and testing for electrical and electronic equipment-Part 2, Electrical loads. (2010).
[162] SAND 2005-3123. Electrical Energy Storage System Abuse Test Manual for Electric and Hybrid Electric Vehicle Applications. 2006
[163] SAND, 99–0497. United States Advanced Battery Consortium Electrochemical Storage System Abuse Test, Procedure Manual. (1999).
[164] SAE, J1715. Hybrid Electric Vehicle (HEV) and Electric Vehicle (EV), Terminology. (2014).
[165] SAE J1739. Potential Failure Mode and Effects Analysis in Design (Design FMEA), Potential Failure Mode and Effects Analysis in Manufacturing and Assembly Processes (Process FMEA). 2009.
[166] SAE J1950. Proving Ground Vehicle Corrosion Testing. 1989.
[167] SAE, J2344. Guidelines for Electric Vehicle, Safety. (2010).
[168] GB/T 31484. Cycle life requirements and test methods of power batteries for electric vehicles. 2015

[169] GB/T 31486. Electrical performance requirements and test methods of power batteries for electric vehicles. 2015
[170] GB/T 31467.3. Lithium-ion battery packs and systems for electric vehicles Part 3: Safety requirements and test methods. 2015
[171] ISO, 16750–1. Road vehicles-Environmental conditions and testing for electrical and electronic equipment-Part 1, General. (2006).
[172] ISO, 16750–3. Road vehicles-Environmental conditions and testing for electrical and electronic equipment-Part 3, Mechaniccal loads. (2012).
[173] ISO, 16750–4. Road vehicles-Environmental conditions and testing for electrical and electronic equipment-Part 4, Climatic loads. (2010).
[174] ISO, 16750–5. Conditions and testing for electrical and electronic equipment-Part 5, Chemical loads. (2010).

[175] IEC 62660-2, Secondary lithium-ion cells for the propulsion of electric road vehicles-Part 2: Reliability and abuse testing. 2010
[176] IEC, 62660–3. Secondary lithium-ion cells for the propulsion of electric road vehicles-Part 3, Safety requirements. (2016).
[177] IEC, 60068-2-2. Environmental testing-Part 2–2: Tests-Test B, Dry heat. (2007).
[178] UL 1642. Standard for lithium batteries. 2009
[179] UL 2054. Standard for household and commercial batteries. 2009.
[180] GM-Modified USABC. General Motors Battery Test Standard for Electric Vehicles. 2016.
[181] VW PV8450. Volkswagen battery test standards for electric vehicles. 2016.
[182] SMTC 9 N20 011. Electrochemical performance test specification of electric vehicles for lithium-ion battery. 2018.